[AMERICAN JOURNAL OF SCIENCE, VOL. 281, MAY, 1981, P. 576-614]

CHEMICAL INTERACTION OF AQUEOUS SOLUTIONS WITH EPIDOTE–FELDSPAR MINERAL ASSEMBLAGES IN GEOLOGIC SYSTEMS. II. EQUILIBRIUM CONSTRAINTS IN METAMORPHIC/GEOTHERMAL PROCESSES

DENNIS K. BIRD* and HAROLD C. HELGESON

Department of Geology and Geophysics, University of California, Berkeley, California 94720

ABSTRACT. Thermodynamic analysis of the system Na_2O–K_2O–CaO–FeO–Fe_2O_3–Al_2O_3–SiO_2–H_2O–HCl–CO_2 at pressures and temperatures to 5 kb and 600°C affords quantitative description and interpretation of phase relations among epidote, garnet, plagioclase, and alkali feldspar solid solutions in hydrothermal systems. Comparison of computed and observed compositions of these minerals and coexisting fluids suggests that the calculations afford close approximation of equilibrium and mass transfer in metamorphic/geothermal processes. The standard molal enthalpies of decomposition reactions for plagioclase are of the order of −4 to −50 kcal mole^{-1}, which requires the activity of the anorthite component of plagioclase coexisting with epidote solid solutions to increase with increasing temperature at constant pressure. In contrast, because the standard molal volumes of these reactions are also negative, $a_{CaAl_2Si_2O_8}$ decreases with increasing pressure at constant temperature. Stoichiometric clinozoisite is stable in the presence of plagioclase and an aqueous phase over a wide range of $a_{CaAl_2Si_2O_8}$ as well as $a_{Ca^{++}}/a_{H^+}^2$, $a_{Al^{+++}}/a_{H^+}^3$, and $a_{Fe^{+++}}/a_{H^+}^3$ in the aqueous solution. However, increasing Fe^{+++} substitution for Al^{+++} to form epidote solid solutions decreases dramatically the range of coexisting plagioclase and fluid compositions. Either stoichiometric epidote or clinozoisite is compatible with plagioclase, quartz, calcite, and an aqueous phase, but only at $X_{CO_2} \lesssim 0.2$. The complex zoning commonly exhibited by both plagioclase and epidote solid solutions in geologic systems can be attributed to minor isothermal/isobaric changes in the composition of coexisting aqueous solutions. Logarithmic activity and fugacity diagrams constructed with provision for solid solution permit documentation of such changes and facilitate thermodynamic interpretation of mineral and fluid compositions in metamorphic/geothermal systems.

INTRODUCTION

Analysis of the compositions of coexisting epidote and feldspar solid solutions facilitates correlation of phase relations with temperature, pressure, and the chemical potentials of the thermodynamic components of metamorphic/geothermal systems.[1] For example, field and laboratory observations indicate that the anorthite content of plagioclase coexisting with epidote solid solutions increases with increasing metamorphic grade (Ramberg, 1943, 1944, 1949, 1952; Rosenqvist, 1952; Turner, 1948; Barth, 1952; Fyfe, Turner, and Verhoogen, 1958; de Waard, 1959; Wenk, 1962; Holdaway, 1965; Crawford, 1966; Wenk and Keller, 1969; Orville and Johannes, 1972; Ghent and DeVries, 1972; Rambaldi, 1973; Hörmann and Raith, 1973; Morteani and Raase, 1974; Höy, 1976; Goldsmith, 1978). Similarly, the occurrence and compositions of coexisting epidote solid solutions and alkali feldspars in geothermal reservoirs have been shown to

* Present address, Department of Geosciences, University of Arizona, Tucson, Arizona 85721

[1] The terms epidote, K-feldspar, and albite are used in the present communication to refer to $Ca_2FeAl_2Si_3O_{12}(OH)$, $KAlSi_3O_8$, and $NaAlSi_3O_8$ in their stable states of order/disorder. Solid solutions of epidote–clinozoisite and andradite–grossular are referred to as epidote and grandite garnet solid solutions, respectively.

be functions of both depth and temperature (White and Sigvaldason, 1961; Muffler and White, 1969; McDowell and McCurry, 1977; Hoagland and Elders, 1978; Kendall, ms). Although correlations of this kind have been largely qualitative in the past, they can now be rendered quantitative by taking account of recent advances in theoretical geochemistry. These advances permit comprehensive calculation of the thermodynamic properties of aqueous species, minerals, and gases at high pressures and temperatures (Helgeson and Kirkham, 1974a and b, 1976; Helgeson, Kirkham, and Flowers, 1981; Walther and Helgeson, 1977, 1980; Delany and Helgeson, 1978; Helgeson and others, 1978; Bird and Helgeson, 1977, 1980; Flowers, 1979; McKenzie and Helgeson, 1979, 1980; Helgeson, 1981). The purpose of the present communication is twofold: (1) to characterize with the aid of such calculations various chemical and thermodynamic constraints imposed by equilibrium among epidote, garnet, and feldspar solid solutions in geologic systems, and (2) to assess the dependence of compositional variation in these minerals on pressure, temperature, and the compositions of coexisting fluids.

The compositions and compatibilities of epidote solid solutions, plagioclase, garnet, laumontite, lawsonite, prehnite, wollastonite, and other minerals in the systems CaO–Na_2O–Fe_2O_3–Al_2O_3–SiO_2–H_2O–CO_2 are common discriminators in classifications of metamorphic rocks (Eskola, 1920; Ramberg, 1949; Rosenqvist, 1952; Turner, 1948, 1968; Misch, 1968; Seki, 1972; Winkler, 1974). Most such classifications are based in part on observations of coexisting plagioclase and epidote solid solutions as a function of pressure, temperature, and fluid composition. For example, Ramberg (1949, 1952), Rosenqvist (1952), Kretz (1963), and Lindh (1978) applied the phase rule in this context to assess the relative stabilities of various mineral assemblages in the system Na_2O–K_2O–CaO–FeO–Fe_2O_3–Al_2O_3–SiO_2–H_2O–CO_2. Similarly, the compatibilities and compositions of coexisting epidote and plagioclase or alkali feldspar solid solutions are commonly used to estimate relative temperatures and fluid compositions in both metamorphic and geothermal processes (Ghent and DeVries, 1972; Orville and Johannes, 1972; Frey and Orville, 1974; Höy, 1976; Kerrick, 1977; Helgeson, 1967; Browne and Ellis, 1970). The extent to which long- and short-range order in plagioclase affects the equilibrium compositions of coexisting aqueous fluids and epidote solid solutions has been assessed in terms of the mixing properties of $NaAlSi_3O_8$ and $CaAl_2Si_2O_8$, metastable order/disorder, and transient pressure/temperature conditions during metamorphism (Christie, 1959, 1962; Rutland, 1961, 1962; Noble, 1962; Brown, 1962; Sen, 1963; Orville, 1974; Wenk and Wenk, 1977; Wenk, 1977; and others). However, the metasomatic consequences of substitutional order/disorder and compositional variation in epidote solid solutions have been largely overlooked.

Phase relations among aqueous solutions and minerals in the system CaO–FeO–Fe_2O_3–Al_2O_3–SiO_2–H_2O–HCl–CO_2 at pressures and temperatures to 5 kb and 600°C are described below with the aid of pressure-temperature, temperature-composition, and logarithmic activity and fugac-

ity diagrams which include provision for both solid solution and substitutional order/disorder in minerals. The stability field boundaries in these diagrams were generated for fluid pressure (P_{fluid}) equal to total pressure (P_{total}) using thermodynamic equations and data given by Helgeson and others (1978), Helgeson and Kirkham (1974a), Helgeson, Kirkham, and Flowers (1981), Walther and Helgeson (1977), Bird and Helgeson (1980), and Flowers (1979).[2] Because the transition from clinozoisite to zoisite is sluggish and has not been reversed experimentally, the latter polymorph was not considered in the calculations. The thermodynamic data adopted for clinozoisite were estimated by Helgeson and others (1978) from experimental observations reported by Holdaway (1972) and Dexter Perkins, III (1977, written commun.). The thermodynamic data given by Helgeson and others (1978) for margarite, lawsonite, and grossular are compatible with recent calorimetric data (Perkins, Westrum, and Essene, 1980; Haselton and Westrum, 1980), but those for prehnite are not (see below).

The standard state for liquids and the intercrystalline standard state for solids employed in the present study correspond to unit activity of the pure component at any pressure and temperature. The intracrystalline standard state for solids requires all activity coefficients of atoms on the lattice sites of solid solutions to approach unity as the mole fractions of the atoms on the sites approach those in the thermodynamic components of the solutions. The standard state for gases is one of unit fugacity of the hypothetical perfect gas at 1 bar and any specified temperature, and that for aqueous species other than H_2O calls for unit activity of the species in a hypothetical 1 molal solution referenced to infinite dilution at any pressure and temperature.

PHASE RELATIONS AMONG AQUEOUS SOLUTIONS AND STOICHIOMETRIC MINERALS IN THE SYSTEM CaO–Al_2O_3–SiO_2–H_2O–HCl–CO_2

Description and interpretation of phase relations in this system requires simultaneous consideration of the extent to which pressure, temperature, and the composition of the aqueous phase affect the compositions and compatibilities of a wide variety of minerals. As a consequence, analysis of phase relations among stoichiometric minerals in the system affords a convenient point of departure for later consideration of the thermodynamic consequences of compositional variation and substitutional order/disorder.

The subsystem CaO–Al_2O_3–SiO_2–HCl–H_2O.—Equilibrium phase relations among aqueous solutions, quartz, and other stoichiometric min-

[2] Footnote *l* of table 1 in Walther and Helgeson (1977) contains a typographical error which should be corrected. Instead of 49.003 and 31.208 cal mole^{-1} (°K)$^{-1}$, the values shown in the footnote for the standard molal entropies of $Si_{(c)}$ and $O_{2(g)}$ should read 4.5 and 49.003 cal mole^{-1} (°K)$^{-1}$, respectively. In addition, eq (10) in the sentence preceding eq (25) should read eq (13), the second left parenthesis in the third term on the right side of eq (25) should be deleted, and the units of a_s and c_i on page 1330 should be corrected to read cal mole^{-1} bar^{-1} and cal mole^{-1} (°K)$^{-1}$, respectively. It should also be noted that all the calculations discussed above took into account typographical errors in a number of the equations given by Helgeson and Kirkham (1974a and b, 1976), which are corrected in footnote 1 of Helgeson and Kirkham (1976), footnotes 1 and 2 of Walther and Helgeson (1977), footnote 1 of Delany and Helgeson (1978), and footnote 1 of Helgeson (1981).

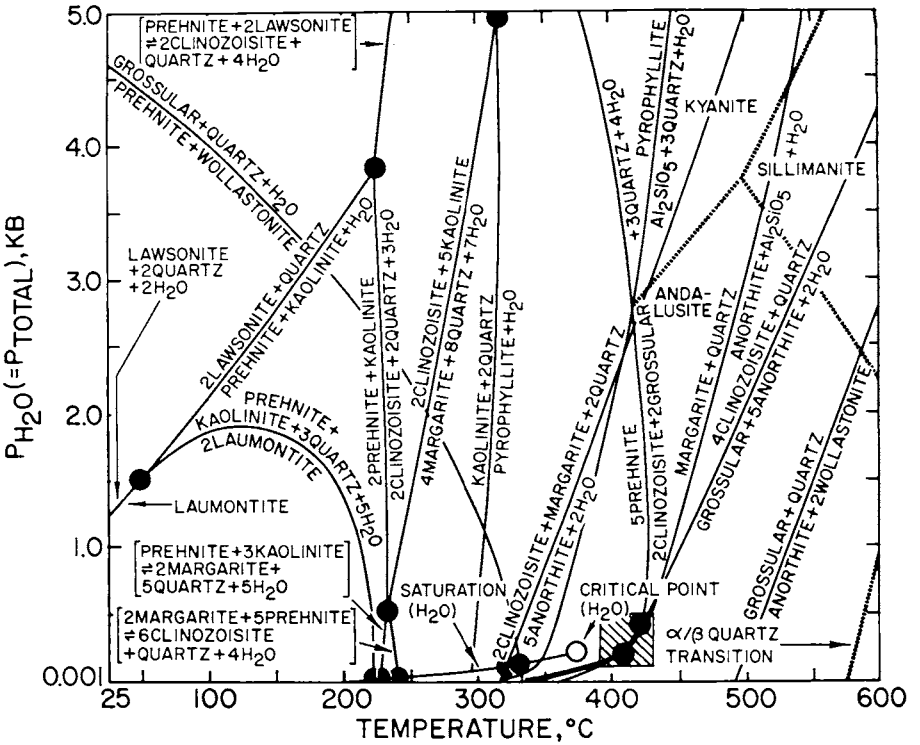

Fig. 1. Phase relations in the system $CaO–Al_2O_3–SiO_2–H_2O$ as a function of pressure and temperature. The solid curves represent univariant reactions in the presence of quartz and an aqueous solution. The dashed curves correspond to phase transitions for Al_2SiO_5 and SiO_2 polymorphs. Saturation (H_2O) refers to the liquid-vapor equilibrium curve for H_2O. The solid symbols represent invariant points, and the hatched area corresponds to the enlargement shown in figure 2.

erals in this system are shown as a function of pressure and temperature in figure 1, where it can be seen that clinozoisite, quartz, and an aqueous phase are compatible over a wide range of temperature and pressure. The reversible dehydration of clinozoisite in the presence of quartz at high pressures and temperatures can be expressed as[3]

$$\underset{(clinozoisite)}{4\ Ca_2Al_3Si_3O_{12}(OH)} + \underset{(quartz)}{SiO_2} \rightleftharpoons \underset{(grossular)}{Ca_3Al_2Si_3O_{12}} + 5\ \underset{(anorthite)}{CaAl_2Si_2O_8} + 2\ H_2O \qquad (1)$$

However, near the critical region for H_2O where grossular is not stable

[3] All reactions other than those shown in the figures (see below) are written in terms of formulas corresponding to the thermodynamic components of minerals, gases, and/or aqueous species. Where the components in the reaction represent stoichiometric minerals, the mineral names are shown in parentheses below the formulas of the components. However, if a formula refers to a component of a solid solution adduced in the text, no name is given beneath the formula. Stoichiometric minerals are represented in reactions shown in the figures by the names of the minerals, but components of solid solutions are designated as they are in the text.

in the presence of clinozoisite and quartz, the latter two minerals coexist with anorthite and prehnite, which can be described by writing

$$\underset{(clinozoisite)}{2\ Ca_2Al_3Si_3O_{12}(OH)} + \underset{(quartz)}{SiO_2} \rightleftharpoons \underset{(anorthite)}{2\ CaAl_2Si_2O_8} + \underset{(prehnite)}{Ca_2Al(AlSi_3O_{10})(OH)_2} \quad (2)$$

The univariant curve representing reaction (2) is shown in figure 2, which is an enlargement of the hatched area in figure 1.

It can be seen in figure 1 that the low-temperature stability of clinozoisite and quartz in the presence of an aqueous solution at pressures < 0.5 kb is controlled by the reaction

$$\underset{(margarite)}{2\ CaAl_2(Al_2Si_2O_{10})(OH)_2} + \underset{(prehnite)}{5\ Ca_2Al(AlSi_3O_{10})(OH)_2} \rightleftharpoons \underset{(clinozoisite)}{6\ Ca_2Al_3Si_3O_{12}(OH)} + \underset{(quartz)}{SiO_2} + 4\ H_2O, \quad (3)$$

which is replaced at $0.5 < P < 3.8$ kb by

$$\underset{(prehnite)}{2\ Ca_2Al(AlSi_3O_{10})(OH)_2} + \underset{(kaolinite)}{Al_2Si_2O_5(OH)_4} \rightleftharpoons \underset{(clinozoisite)}{2\ Ca_2Al_3Si_3O_{12}(OH)} + \underset{(quartz)}{2\ SiO_2} + 3\ H_2O\ . \quad (4)$$

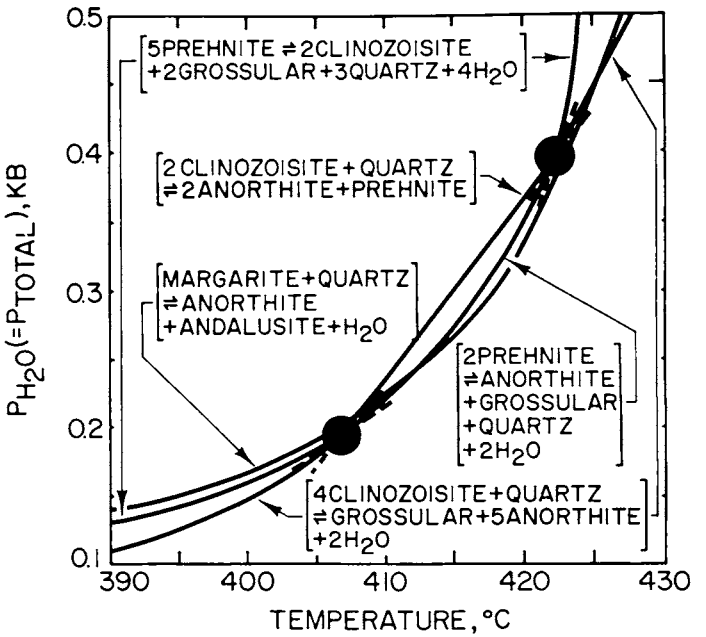

Fig. 2. Phase relations in the system CaO–Al_2O_3–SiO_2–H_2O as a function of pressure and temperature in the presence of quartz and an aqueous solution (see caption of fig. 1).

At high pressures (> 3.8 kb) the reaction limiting the stability of clinozoisite and quartz in the presence of an aqueous phase corresponds to

$$2\,CaAl_2Si_2O_7(OH)_2 \cdot H_2O + Ca_2Al(AlSi_3O_{10})(OH)_2 \rightleftharpoons 2\,Ca_2Al_3Si_3O_{12}(OH) + SiO_2 + 4\,H_2O\,. \quad (5)$$

(*lawsonite*) (*prehnite*) (*clinozoisite*) (*quartz*)

In contrast to the high-temperature decomposition of clinozoisite and quartz represented by reactions (1) and (2), the low-temperature stability of this assemblage (reactions 3, 4, and 5) is essentially independent of pressure at $P_{H_2O} = P_{total} < 5$ kb (fig. 1).

Calcium aluminum silicates that are compatible with quartz and an aqueous phase at temperatures below ~ 225°C (where clinozoisite is not stable in the presence of quartz and an aqueous solution) include lawsonite and grossular at high pressures and prehnite and laumontite at low pressures. It can be seen in figure 1 that laumontite, which is stable only at low temperatures and pressures, cannot coexist with clinozoisite in the presence of quartz and an aqueous solution. Note that the stability field corresponding to prehnite + kaolinite + quartz coexisting with an aqueous phase appears as an irregular wedge which truncates the laumontite stability field at low pressures. However, it should perhaps be emphasized in this regard that the phase relations involving prehnite in figures 1 and 2 represent provisional approximations, owing to relatively large uncertainties in the thermodynamic properties of prehnite (see below).

The standard molal entropies and heat capacities of margarite and lawsonite used to generate the phase relations shown in figures 1 and 2 (Helgeson and others, 1978) differ slightly from the recent calorimetric data reported by Perkins, Westrum, and Essene (1980). Nevertheless, in most instances the differences have a negligible effect on calculated equilibrium temperatures for coexisting minerals in the system CaO–Al_2O_3–SiO_2–H_2O. For example, the univariant curve representing equilibrium among margarite, anorthite, corundum, and H_2O in figure 88 of Helgeson and others (1978) is affected to the extent of only a few degrees by the new calorimetric data. In contrast, an adjustment of -300 cal mole^{-1} in the standard molal Gibbs free energy and enthalpy of formation from the elements of lawsonite at 298.15°K and 1 bar is required for the curve representing equilibrium among lawsonite, laumontite, quartz, and H_2O in figure 91C of Helgeson and others (1978) to be consistent with the entropy and heat capacity data for lawsonite reported by Perkins, Westrum, and Essene (1980). However, such an adjustment affects only slightly (by < 10°K) the univariant curves shown in figures 92B and C of Helgeson and others (1978) corresponding to lawsonite and quartz coexisting with wairakite or zoisite, H_2O, and andalusite, sillimanite, or kyanite, and the curves would still satisfy the experimental reversal temperatures shown in the figures. As a consequence, all the phase relations discussed below are affected negligibly by the new calorimetric data for lawsonite.

The estimated standard molal heat capacities of prehnite adopted in the present study (Helgeson and others, 1978) are in close agreement with the recent experimental values reported by Perkins, Westrum, and Essene (1980). In contrast, the corresponding values of the standard molal entropy of prehnite at 298.15°K and 1 bar differ by ~ 5 cal mole^{-1}(°K)$^{-1}$. The discrepancy arises from Clapeyron slope constraints imposed by the distribution of Liou's (1971) experimental high pressure/temperature phase equilibrium data for the decomposition of prehnite to zoisite, grossular, quartz, and H_2O (Helgeson and others, 1978), which is inconsistent with the calorimetric entropy of prehnite given by Perkins, Westrum, and Essene (1980). The latter data require decomposition of prehnite solid solutions to quartz, H_2O, and garnet and epidote solid solutions at temperatures too low to be consistent with the observed compositions of these minerals in geothermal systems. In contrast, the thermodynamic properties of prehnite adopted by Helgeson and others (1978) afford close agreement between predicted and observed phase relations in geothermal systems (Bird and Helgeson, 1977). It can be shown that the same observation holds for the thermodynamic data given by Helgeson and others (1978),

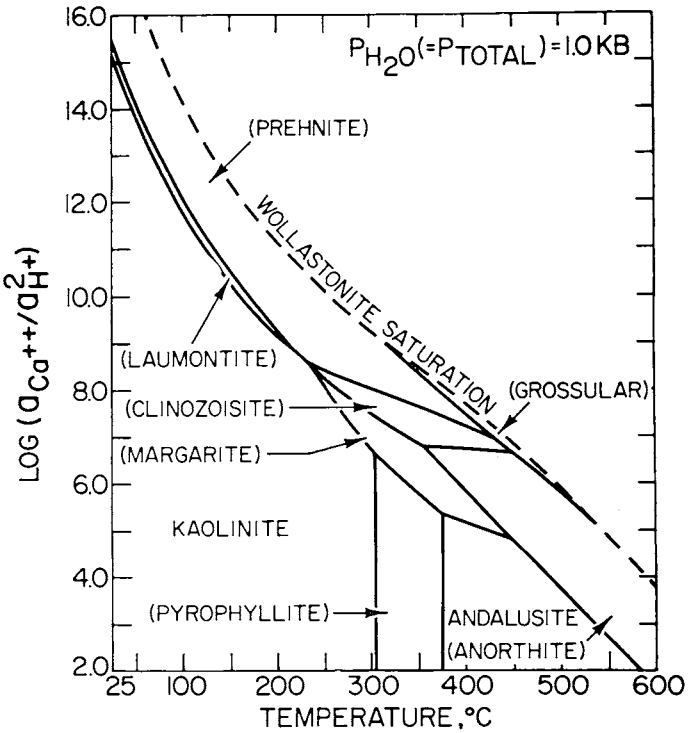

Fig. 3. Phase relations in the system CaO–Al_2O_3–SiO_2–HCl–H_2O in the presence of quartz and an aqueous solution in which $a_{H_2O} \approx 1$ as a function of temperature and log ($a_{Ca^{++}}/a_{H^+}^2$) in the aqueous phase at 1 kb. The dashed curve represents saturation of the fluid phase with respect to wollastonite.

Bird and Helgeson (1980), and Haselton and Westrum (1980) for epidote, andradite, and grossular, but not for the corresponding data reported for these minerals by Aranovich (1976) and Perchuk and Aranovich (1979).

Equilibrium phase relations among minerals in the system CaO–Al_2O_3–SiO_2–H_2O are shown in figures 3 and 4 as a function of temperature and $a_{Ca^{++}}/a_{H^+}{}^2$ in the aqueous phase at 1 and 5 kb. It can be seen in these figures that the range in temperature and $a_{Ca^{++}}/a_{H^+}{}^2$ corresponding to equilibrium among clinozoisite, quartz, and an aqueous solution increases with increasing pressure. For example, at 1 kb (fig. 3) clinozoisite and quartz coexist with an aqueous phase between 230° and 450°C at log $(a_{Ca^{++}}/a_{H^+}{}^2)$ between 8.6 and 6.6. However, at 5 kb (fig. 4) the assemblage is stable from 240° to > 600°C at log $(a_{Ca^{++}}/a_{H^+}{}^2)$ from 8.9 to 6.1. Note that $a_{Ca^{++}}/a_{H^+}{}^2$ in an aqueous solution coexisting with clinozoisite, quartz, and anorthite is essentially independent of temperature at low pressures (fig. 3), but at high pressures where the standard molal enthalpy of the reaction is positive, $a_{Ca^{++}}/a_{H^+}{}^2$ increases with increasing temperature (fig. 4). The effect of compositional variation in plagioclase on these observations is considered in a later discussion.

The dependence of phase relations among calcium aluminum silicates on the activity of $SiO_{2(aq)}$ in the coexisting aqueous solution is shown in

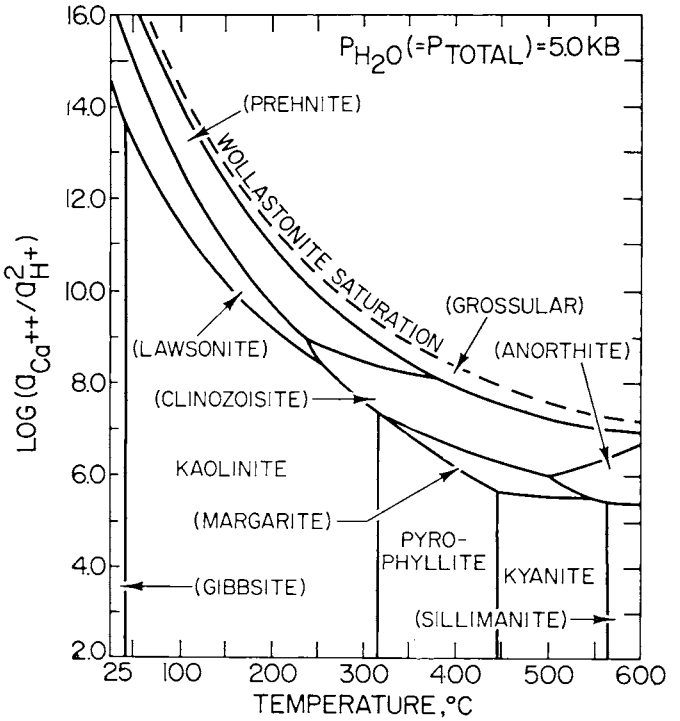

Fig. 4. Phase relations in the system CaO–Al_2O_3–SiO_2–HCl–H_2O in the presence of quartz and an aqueous solution in which $a_{H_2O} \approx 1$ as a function of temperature and log $(a_{Ca^{++}}/a_{H^+}{}^2)$ in the aqueous phase at 5 kb (see caption of fig. 3).

figure 5, where it can be seen that the size of the anorthite stability field decreases dramatically relative to those of clinozoisite and margarite with decreasing values of $a_{SiO_2(aq)}$. Note also in this figure that stoichiometric wairakite cannot coexist with an aqueous solution at 1 kb and 400°C unless the aqueous phase is supersaturated with respect to quartz. This observation is also true for all other pressures $< P_{H_2O} = P_{total} = 5$ kb and temperatures < 600°C (fig. 1). However, it can be shown that compositional variation leading to wairakite solid solutions in which $a_{CaAl_2Si_4O_{12} \cdot 2\,H_2O} \leqslant 0.93$ at 1 kb and 400°C enlarges the wairakite stability field enough to include fluid compositions compatible with quartz.

The subsystem CaO–Al_2O_3–SiO_2–H_2O–CO_2.—Phase relations among stoichiometric minerals in this system are shown in figures 6 and 7 as a function of temperature and fluid composition at $P_{fluid} = P_{total} = 1$ and 5 kb, respectively. The dashed curves in these figures represent ideal mixing of H_2O and CO_2, but the solid curves were generated using equations summarized by Flowers (1979) for nonideal mixing in the system H_2O–CO_2.

It can be seen in figures 6 and 7 that clinozoisite, prehnite, grossular, and wollastonite coexist only with H_2O-rich solutions from 400° to 600°C at 1 and 5 kb, but margarite and anorthite are stable over a wide range

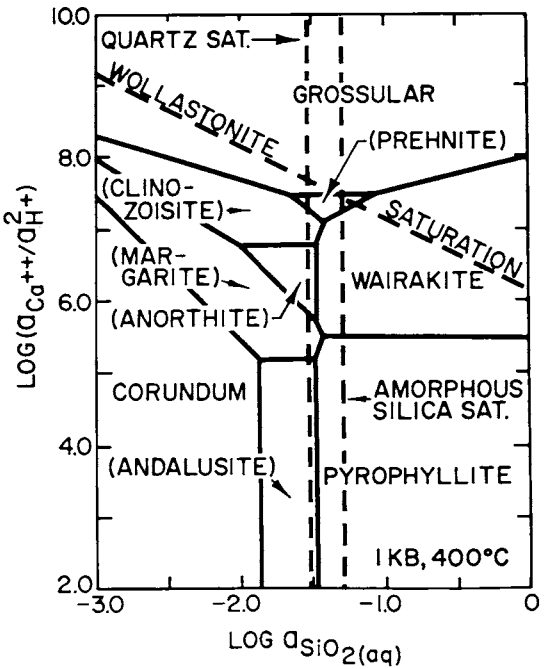

Fig. 5. Phase relations in the system CaO–Al_2O_3–SiO_2–HCl–H_2O for $a_{H_2O} \approx 1$ as a function of log $(a_{Ca^{++}}/a_{H^+}^2)$ and log $a_{SiO_2(aq)}$ in the aqueous phase at 1 kb and 400°C. The dashed curves represent saturation of the fluid phase with respect to wollastonite, quartz, or amorphous silica.

of X_{CO_2}. Comparison of the curves shown in the figures for ideal and nonideal mixing in the system H_2O–CO_2 leaves little doubt that computed equilibrium temperatures and fluid compositions for coexisting calcium-aluminum silicates are sensitive to the mixing equations used in the calculations. Similar observations have been made by Kerrick and Jacobs (1978).

THERMODYNAMIC CONSEQUENCES OF COMPOSITIONAL VARIATION IN EPIDOTE, PLAGIOCLASE, AND GARNET SOLID SOLUTIONS AT HIGH PRESSURES AND TEMPERATURES

Equilibrium among epidote solid solutions, plagioclase, and an aqueous phase in the system CaO–Na_2O–Fe_2O_3–Al_2O_3–SiO_2–HCl–H_2O can be described by writing

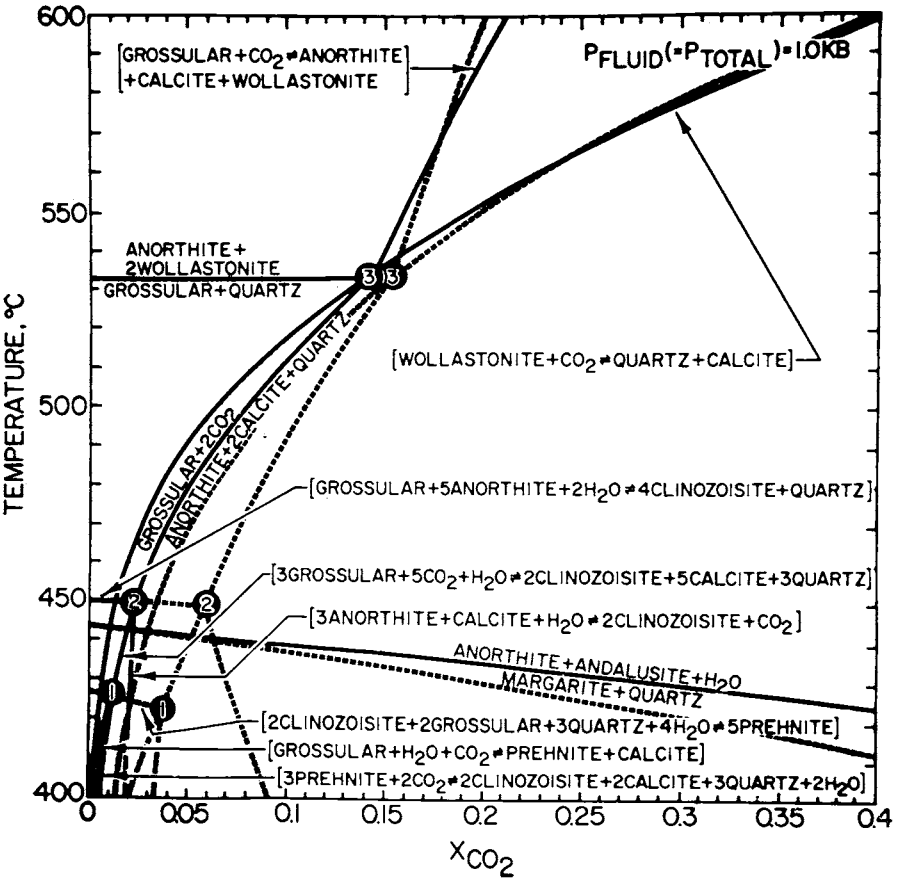

Fig. 6. Phase relations in the system CaO–Al_2O_3–SiO_2–H_2O–CO_2 as a function of temperature and X_{CO_2} at 1 kb. The solid curves represent nonideal mixing of H_2O and CO_2 computed from equations given by Flowers (1979), but the dotted curves correspond to ideal mixing of these components. The numbered symbols designate positions of corresponding isobaric invariant points for the two types of mixing approximations used to generate the diagram (see text).

$$2\ Ca_2Al_3Si_3O_{12}(OH) + 2\ H^+ \rightleftharpoons 3\ CaAl_2Si_2O_8 + Ca^{++} + 2\ H_2O\ , \qquad (6)$$

and

$$Ca_2FeAl_2Si_3O_{12}(OH) + 5\ H^+ \rightleftharpoons CaAl_2Si_2O_8 + Ca^{++} + Fe^{+++} + SiO_{2(aq)} + 3\ H_2O\ . \qquad (7)$$

The laws of mass action for reactions (6) and (7) appear as

$$K = (a_{CaAl_2Si_2O_8})^3\ (a_{Ca_2Al_3Si_3O_{12}(OH)})^{-2}\ (a_{Ca^{++}}/a_{H^+}{}^2)\ (a_{H_2O})^2 \qquad (8)$$

and

$$K = (a_{CaAl_2Si_2O_8})\ (a_{Ca_2FeAl_2Si_3O_{12}(OH)})^{-1}\ (a_{Ca^{++}}/a_{H^+}{}^2) \cdot (a_{Fe^{+++}}/a_{H^+}{}^3)\ (a_{SiO_{2(aq)}})\ (a_{H_2O})^3 \qquad (9)$$

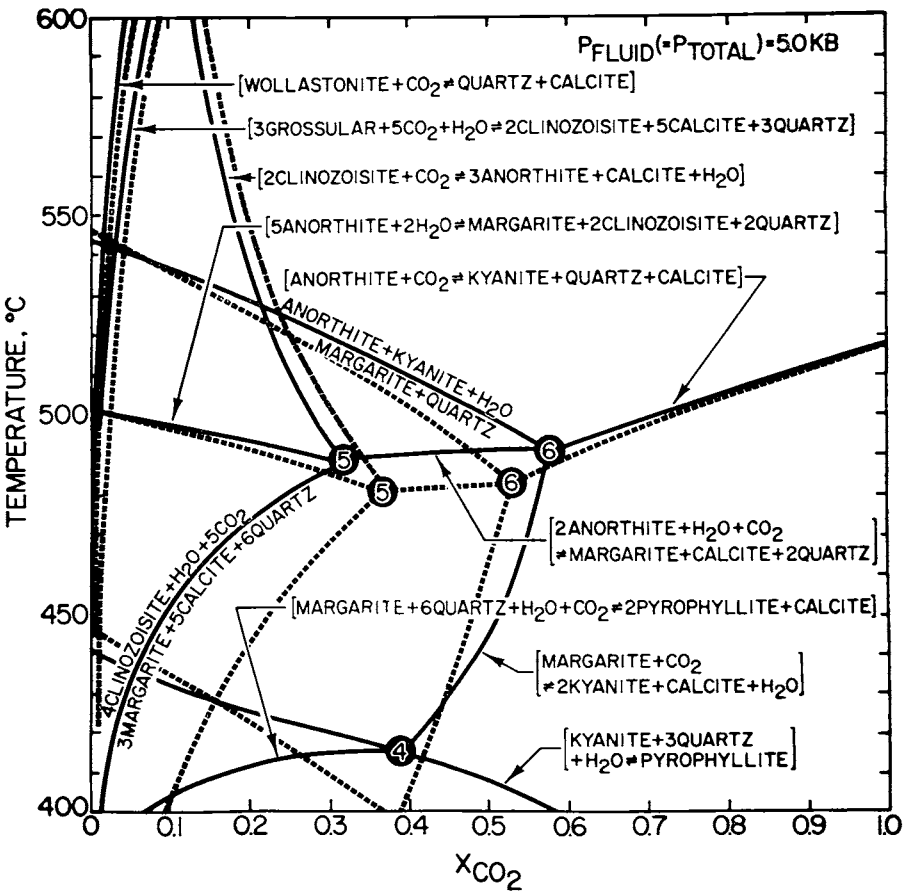

Fig. 7. Phase relations in the system CaO–Al_2O_3–SiO_2–H_2O–CO_2 as a function of temperature and X_{CO_2} at 5 kb (see caption of fig. 6).

respectively, where K denotes the equilibrium constants for the respective reactions, $a_{CaAl_2Si_2O_8}$ represents the activity of the anorthite component of plagioclase, and $a_{Ca_2FeAl_2Si_3O_{12}(OH)}$ and $a_{Ca_2Al_3Si_3O_{12}(OH)}$ correspond to the activities of the epidote and clinozoisite components of the epidote solid solution. The latter two activities are related to composition and temperature by equations and data given by Bird and Helgeson (1980), but the activity of the anorthite component of plagioclase is related to composition by

$$a_{CaAl_2Si_2O_8} = (X_{CaAl_2Si_2O_8})(\lambda_{CaAl_2Si_2O_8}) \tag{10}$$

where $X_{CaAl_2Si_2O_8}$ and $\lambda_{CaAl_2Si_2O_8}$ stand for the mole fraction and activity coefficient of the subscripted component, respectively. The activities of aqueous species other than H_2O in eqs (8) and (9) are related to concentration by

$$a_i = m_i\bar{\gamma}_i \tag{11}$$

where m_i and $\bar{\gamma}_i$ refer to the molality and activity coefficient of the ith aqueous species, respectively.

The coexistence of plagioclase and an aqueous phase can be represented by writing

$$CaAl_2Si_2O_8 + 2\,Na^+ + 4\,SiO_{2(aq)} \rightleftharpoons 2\,NaAlSi_3O_8 + Ca^{++} \tag{12}$$

for which

$$a_{Na^+} = \left(a_{Ca^{++}} (a_{SiO_{2(aq)}})^{-4}\, K^{-1} \left(\frac{a_{NaAlSi_3O_8}{}^2}{a_{CaAl_2Si_2O_8}} \right) \right)^{0.5} \tag{13}$$

where K stands for the equilibrium constant for reaction (12), and $a_{NaAlSi_3O_8}$ corresponds to the activity of the albite component of plagioclase, which is related to composition by

$$a_{NaAlSi_3O_8} = (1 - X_{CaAl_2Si_2O_8})(\lambda_{NaAlSi_3O_8})\,. \tag{14}$$

where $\lambda_{NaAlSi_3O_8}$ stands for the activity coefficient of the albite component of plagioclase.

Although high concentrations of electrolytes may occur in aqueous solutions involved in metamorphic processes, the activity of H_2O relative to the liquid standard state is commonly close to unity (Helgeson, 1967, 1969, 1981; Helgeson and others, 1978). Accordingly, the phase relations among minerals and aqueous solutions presented below were generated for $a_{H_2O} = 1$, except for systems involving CO_2. Nonideal mixing approximations for H_2O and CO_2 taken from Flowers (1979) were used in the latter cases to compute the positions of stability field boundaries.

Experimental observations of plagioclase solid solutions at high pressures and temperatures by Orville (1972) and Windom and Boettcher (1976) indicate that small positive deviations from ideality occur ($1.0 < \lambda_{CaAl_2Si_2O_8} \lesssim 1.3$) at 700°C and 2 kb, and at 1100°C and pressures > 14 kb. Nevertheless, the consequences of short- and long-range order/disorder in plagioclase results in numerous compositional and structural discontinuities at lower pressures and temperatures, many of which have been

documented in metamorphic systems (Evans, 1964; Wenk, 1962; Crawford, 1966, 1972; Nissen, 1974; Wenk and others, 1975; Grove, 1976; Steck, 1976; Wenk and Wenk, 1977; Wenk, 1977; Garrison, 1978; and others). In general, activity/composition relations such as those proposed by Saxena and Ribbe (1972) and Kerrick and Darken (1975) fail to account adequately for these observations. Accordingly, no attempt was made in the present study to calculate numerical values of $X_{CaAl_2Si_2O_8}$ from $a_{CaAl_2Si_2O_8}$.

Phase relations among anorthite and other minerals in the system CaO–Fe_2O_3–FeO–Al_2O_3–SiO_2–H_2O–CO_2.—Analysis of phase relations in this system requires provision for both compositional variation and substitutional order/disorder among octahedral Fe^{+++} and Al^{+++} in grandite garnet and epidote solid solutions. Activity/composition relations and site occupancies in these minerals were computed from equations and data given by Bird and Helgeson (1980).

The effect of compositional variation in grandite garnet and epidote solid solutions on the composition of coexisting aqueous solutions is depicted in figure 8. The isopleths corresponding to constant $X_{Ca_2Fe_3Si_3O_{12}(OH)}$ in figures 8A and B represent equilibrium among epidote solid solutions, quartz, and an aqueous phase, which can be described in terms of

$$3\,Ca_2FeAl_2Si_3O_{12}(OH) + 13\,H^+ \rightleftharpoons 2\,Ca_2Al_3Si_3O_{12}(OH) + 3\,SiO_2\,(quartz) + 3\,Fe^{+++} + 2\,Ca^{++} + 7\,H_2O \quad (15)$$

and

$$Ca_2FeAl_2Si_3O_{12}(OH) + Al^{+++} \rightleftharpoons Ca_2Al_3Si_3O_{12}(OH) + Fe^{+++}. \quad (16)$$

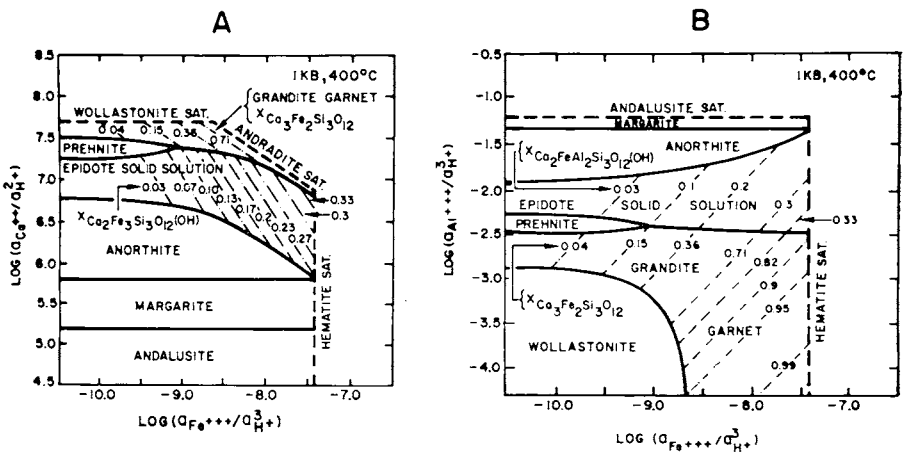

Fig. 8. Phase relations in the system CaO–Fe_2O_3–Al_2O_3–SiO_2–HCl–H_2O in the presence of quartz and an aqueous solution in which $a_{H_2O} \approx 1$ as a function of log ($a_{Ca^{++}}/a_{H^+}^2$), log ($a_{Fe^{+++}}/a_{H^+}^3$), and log ($a_{Al^{+++}}/a_{H^+}^3$) in the aqueous phase at 400°C and 1 kb. The dashed curves represent saturation of the fluid phase with respect to wollastonite, andradite, andalusite, or hematite, but the dot-dash curves denote compositions of epidote and grandite garnet solid solutions.

In contrast, the isopleths corresponding to constant $X_{Ca_3Fe_2Si_3O_{12}}$ in these figures represent equilibrium among grandite garnet solid solutions, quartz, and an aqueous phase, consistent with

$$Ca_3Fe_2Si_3O_{12} + 12\ H^+ \rightleftharpoons 3\ Ca^{++} + 2\ Fe^{+++} + 3\ \underset{(quartz)}{SiO_2} + 6\ H_2O \tag{17}$$

and

$$Ca_3Fe_2Si_3O_{12} + 2\ Al^{+++} \rightleftharpoons Ca_3Al_2Si_3O_{12} + 2\ Fe^{+++}. \tag{18}$$

The compositions shown in figure 8 for coexisting grandite garnet and epidote solid solutions correspond to those for

$$Ca_3Fe_2Si_3O_{12} + 2\ Ca_2Al_2Si_3O_{12}(OH) \rightleftharpoons$$
$$Ca_3Al_2Si_3O_{12} + 2\ Ca_2FeAl_2Si_3O_{12}(OH) \tag{19}$$

It can be seen in figure 8 that equilibrium partitioning of Fe^{+++} and Al^{+++} among grandite garnet and epidote solid solutions (reaction

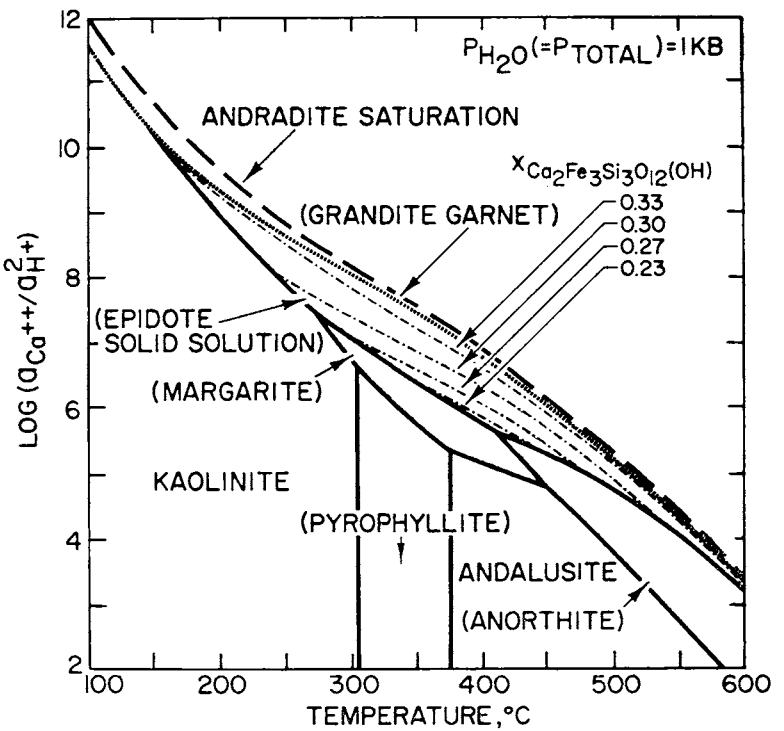

Fig. 9. Phase relations in the system $CaO–Fe_2O_3–Al_2O_3–SiO_2–HCl–H_2O$ in the presence of quartz, hematite, and an aqueous solution in which $a_{H_2O} \approx 1$ as a function of temperature and log $(a_{Ca^{++}}/a_{H^+}^2)$ in the aqueous phase at 1 kb. The dashed curve represents saturation of the fluid phase with respect to andradite, but the dot-dash curves denote epidote solid solution compositions. The dotted curve corresponds to an extrapolation of the stability field boundary separating epidote and grandite garnet solid solutions to $X_{Ca_2Fe_3Si_3O_{12}(OH)} > 0.33$ (see text).

19) leads to decreasing $a_{Ca^{++}}/a_{H^+}{}^2$ and increasing $a_{Fe^{+++}}/a_{H^+}{}^3$ in the aqueous phase with increasing Fe^{+++} substitution for octahedral Al^{+++} in these minerals. However, $a_{Al^{+++}}/a_{H^+}{}^3$ in the aqueous solution is essentially constant and independent of compositional variation in coexisting garnet and epidote solid solutions (fig. 8B). Note that the latter solid solutions are compatible with stoichiometric prehnite, quartz, and an aqueous phase at 1 kb and 400°C only if $X_{Ca_2Fe_3Si_3O_{12}(OH)} \leqslant 0.1$ and $\log (a_{Fe^{+++}}/a_{H^+}{}^3) \leqslant -9.1$. This observation is affected only slightly by minor Fe^{+++} substitution for Al^{+++} in prehnite to form prehnite solid solutions coexisting with either epidote or grandite garnet solid solutions (Bird and Helgeson, 1980). Under the conditions represented by figure 8, epidote solid solutions may coexist with anorthite, quartz, and an aqueous phase at $X_{Ca_2Fe_3Si_3O_{12}(OH)} \leqslant 0.23$ and $\log (a_{Fe^{+++}}/a_{H^+}{}^3) \leqslant -7.4$. Stoichiometric epidote is stable in the presence of quartz and an aqueous phase at 1 kb and 400°C over a narrow range of $a_{Ca^{++}}/a_{H^+}{}^2$, $a_{Al^{+++}}/a_{H^+}{}^3$, and $a_{Fe^{+++}}/a_{H^+}{}^3$ equal to 6.6 to 6.9, −2.5 to −2.2, and −7.6 to −7.4, respectively.

It can be deduced from figure 8 that equilibrium among epidote and grandite garnet solid solutions in the presence of quartz, hematite, and an aqueous phase at 400°C and 1 kb requires $X_{Ca_2Fe_3Si_3O_{12}(OH)} \approx 0.35$ in the pistacite–clinozoisite solid solution. Extrapolation of the composition

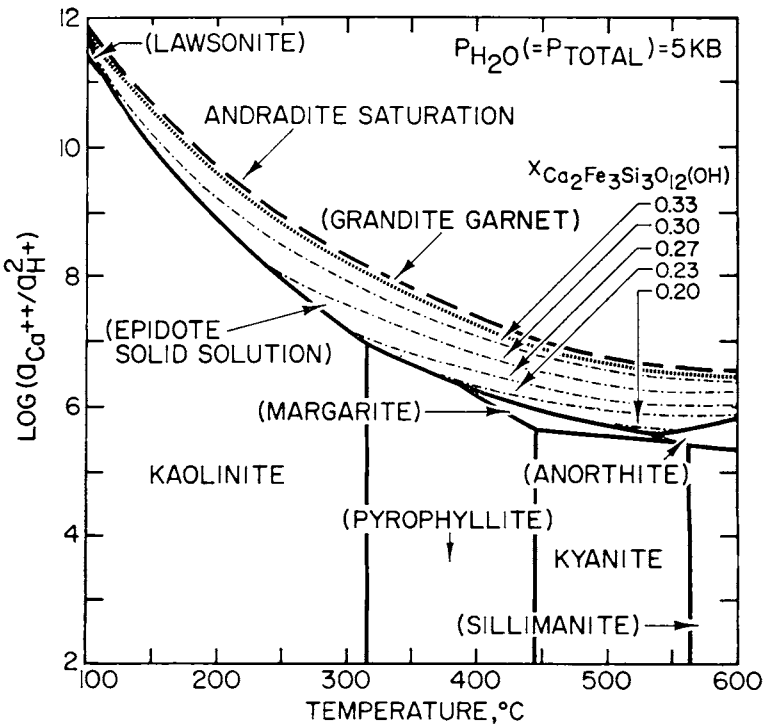

Fig. 10. Phase relations in the system CaO–Fe_2O_3–Al_2O_3–SiO_2–HCl–H_2O in the presence of quartz, hematite, and an aqueous solution in which $a_{H_2O} \approx 1$ as a function of temperature and $\log (a_{Ca^{++}}/a_{H^+}{}^2)$ in the aqueous phase at 5 kb (see caption of fig. 9).

of the coexisting grandite garnet solid solution in figure 15 of Bird and Helgeson (1980) leads to $X_{Ca_3Fe_2Si_3O_{12}} \approx 0.9$. Hematite saturation precludes higher concentrations of $Ca_3Fe_2Si_3O_{12}(OH)$ and $Ca_3Fe_2Si_3O_{12}$ in these solid solutions. However, at higher and lower temperatures, $X_{Ca_2Fe_3Si_3O_{12}(OH)}$ decreases to 0.33 (see below).

Phase relations in the system CaO–Fe_2O_3–Al_2O_3–SiO_2–H_2O in the presence of quartz, hematite, and an aqueous phase are shown in figures 9 and 10 for $P_{H_2O} = P_{total} = 1$ and 5 kb, respectively. The dot-dash curves in the figures represent contours of constant composition for epidote solid solutions computed from the law of mass action for

$$6\ Ca_2FeAl_2Si_3O_{12}(OH) + 8\ H^+ \rightleftharpoons 4\ Ca_2Al_3Si_3O_{12}(OH) + 3\ Fe_2O_3 + 6\ SiO_2 + 4\ Ca^{++} + 5\ H_2O \quad (20)$$

(*hematite*) (*quartz*)

Note that the stability fields of the grandite garnet solid solutions in the two diagrams are vanishingly small compared to those of the epidote solid solutions.

It can be seen in figures 9 and 10 that epidote solid solutions are stable in the presence of quartz and an aqueous phase from $\sim 100°$ to $> 600°$C at 1 and 5 kb. The dramatic effect of compositional variation in epidote on its stability in hydrothermal systems can be assessed by comparing these figures with figures 3 and 4, respectively, where phase relations are portrayed for $X_{Ca_2Fe_3Si_3O_{12}(OH)} = X_{Ca_2Fe_2Si_3O_{12}} = 0$ at 1 and 5 kb. Note that at both high and low temperatures, the composition of epidote solid solutions coexisting with quartz, hematite, and an aqueous phase approaches $X_{Ca_2Fe_3Si_3O_{12}(OH)} = 0.33$, which is consistent with conclusions reached independently by Miyashiro and Seki (1958) and Strens (1965) from petrologic and experimental observations. The minimum values of $X_{Ca_2Fe_3Si_3O_{12}(OH)}$ shown in figures 9 and 10 represent equilibrium among epidote solid solutions and stoichiometric margarite, anorthite, hematite, quartz, and an aqueous phase at 1 kb and 410°C (where $X_{Ca_2Fe_3Si_3O_{12}(OH)} = 0.22$) and 5 kb and 525°C (where $X_{Ca_2Fe_3Si_3O_{12}(OH)} = 0.18$), respectively. Note that $X_{Ca_2Fe_3Si_3O_{12}(OH)}$ decreases with increasing temperature at temperatures $< 410°$C at 1 kb and $< 525°$C at 5 kb for epidote solid solutions coexisting with stoichiometric kaolinite, pyrophyllite, or margarite. In contrast, $X_{Ca_2Fe_3Si_3O_{12}(OH)}$ increases with increasing temperature at constant pressure for epidote solid solutions coexisting with stoichiometric anorthite.

The effect of compositional variation in epidote solid solutions on the compositions of coexisting fluids in equilibrium with quartz and calcite in the presence of anorthite, grandite garnet, or hematite can be assessed by inspection of figure 11, where phase relations are shown as a function of X_{CO_2} and $\log (a_{Fe^{+++}}/(\sigma_{Fe^{+++}} a_{H^+}{}^3))$ in the fluid phase. $\sigma_{Fe^{+++}}$ in figure 11 (and subsequent figures) provides explicitly for solvation of the subscripted species in accord with (Walther and Helgeson, 1980)

$$\sigma_i \equiv a_{H_2O}{}^{(n_i - Z_i n_{H^+})} \quad (20a)$$

where n_i and Z_i stand for the solvation number and charge of the ith aqueous species. The stability field boundaries shown in figure 11 were generated with the aid of equations and data given by Flowers (1979) describing nonideal mixing in the system H_2O–CO_2. The isopleths corresponding to constant $X_{Ca_2Fe_3Si_3O_{12}(OH)}$ were generated from the law of mass action for

$$6\ Ca_2FeAl_2Si_3O_{12}(OH) + 4\ CO_2 + 18\ H^+ \rightleftharpoons 4\ Ca_2Al_3Si_3O_{12}(OH) + 6\ Fe^{+++} + 4\ \underset{(calcite)}{CaCO_3} + 6\ \underset{(quartz)}{SiO_2} + 10\ H_2O \quad (21)$$

It should perhaps be emphasized in this regard that the equilibrium phase relations shown for coexisting epidote and grandite garnet solid solutions in figure 11 are consistent with Bird and Helgeson's (1980) calculation of the relative extent to which Fe^{+++} and Al^{+++} are partitioned among the various octahedral sites in the two minerals.

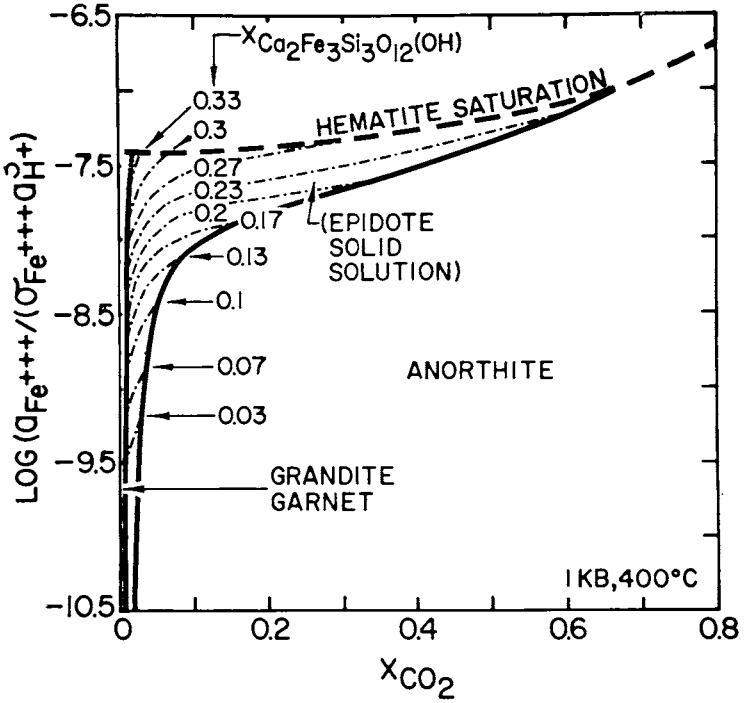

Fig. 11. Phase relations in the system CaO–Fe_2O_3–Al_2O_3–SiO_2–HCl–H_2O–CO_2 in the presence of quartz and calcite as a function of log ($a_{Fe^{+++}}/\sigma_{Fe^{+++}}a_{H^+}^3$) and X_{CO_2} in the fluid phase at 1 kb and 400°C (see text). The dashed curve represents saturation of the fluid phase with respect to hematite, but the dotted curve corresponds to an extrapolation of the stability field boundary separating epidote and grandite garnet solid solutions to $X_{Ca_2Fe_3Si_3O_{12}(OH)} > 0.33$ (see text). The dot-dash curves denote epidote solid solution compositions. The symbol $\sigma_{Fe^{+++}}$ on the ordinate provides explicitly for solvation of aqueous species (Walther and Helgeson, 1980) — see text.

It can be seen in figure 11 that the coexistence of grandite garnet and epidote solid solutions in the presence of calcite, quartz, and a fluid phase is restricted to H_2O-rich solutions ($X_{CO_2} < 0.02$ at 400°C and 1 kb). This observation holds also for clinozoisite-rich epidote solid solutions as well as stoichiometric epidote in the absence of grandite garnet. In contrast, epidote solid solutions of intermediate composition are stable over a wide range of fluid compositions. Convergence of the $X_{Ca_2Fe_3Si_3O_{12}(OH)}$ isopleths at $X_{CO_2} \lesssim 0.05$ in figure 11 leads to a highly sensitive interdependence of the compositions of coexisting epidote solid solutions and H_2O-rich fluids. This sensitivity almost certainly contributes significantly to the complex compositional zoning commonly observed in epidote solid solutions in geologic systems.

The dependence of the equilibrium compositions of coexisting calcium iron aluminum silicates on the activities of Fe^{++} and Fe^{+++} in the aqueous phase can be expressed by taking account of

$$4\,Fe^{+++} + 2\,H_2O \rightleftharpoons 4\,Fe^{++} + O_{2(g)} + 4\,H^+ \tag{22}$$

for which the law of mass action can be written as

$$f_{O_{2(g)}} = K\,(a_{Fe^{+++}}/a_{H^+}{}^3)^4\,(a_{Fe^{++}}/a_{H^+}{}^2)^{-4}\,(a_{H_2O})^2 \tag{23}$$

where $f_{O_{2(g)}}$ represents the fugacity of oxygen gas (indicated by the subscript (g)) in the system.

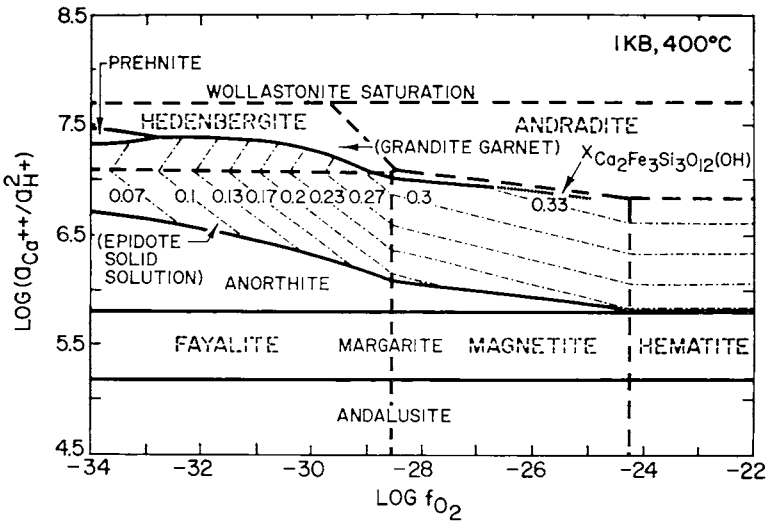

Fig. 12. Phase relations in the system CaO–FeO–Fe_2O_3–Al_2O_3–SiO_2–HCl–H_2O in the presence of quartz and other minerals in the subsystem CaO–FeO–Fe_2O_3–SiO_2 (indicated by the dashed labels) as a function of log f_{O_2} and log $(a_{Ca^{++}}/_{H^+}{}^2)$ in the aqueous phase at 400°C, 1 kb, and $a_{H_2O} \approx 1$. With one exception (see below), the dashed curves represent phase relations in the subsystem CaO–FeO–Fe_2O_3–SiO_2 in the presence of quartz. The stability fields for minerals in this system are superimposed on those delimited by the solid curves. The dashed curve labeled wollastonite saturation represents saturation of the fluid phase with respect to wollastonite. The dot-dash curves denote the compositions of epidote solid solutions.

Phase relations among minerals in the system CaO–FeO–Fe_2O_3–Al_2O_3–SiO_2–H_2O are depicted in figures 12 and 13 as a function of f_{O_2} and $a_{Ca^{++}}/a_{H^+}{}^2$ in the fluid phase. The diagrams shown in these figures represent two superimposed subsystems. The dashed curves delimit stability fields for minerals in the system CaO–Fe_2O_3–FeO–SiO_2 in the presence of quartz and an aqueous solution. The latter stability fields are labeled in the figures with dashed mineral names. The solid curves and labels represent phase relations for minerals in the system CaO–Fe_2O_3–Al_2O_3–SiO_2–H_2O in the presence of quartz, an aqueous phase, and either fayalite, hedenbergite, wollastonite, andradite, magnetite, or hematite. The dearth of reliable thermodynamic data for almandine ($Fe_3Al_2Si_3O_{12}$) precludes calculation of phase relations involving andradite–grossular–almandine solid solutions as well as the consequences of changes in f_{O_2} on compositional variation in coexisting garnet and epidote solid solutions. Nevertheless, the maximum stability of epidote solid solutions can be approximated from the compositions of epidote and coexisting grandite garnet solid solutions computed from equations and data given by Bird and Helgeson (1980).

It can be seen in figures 12 and 13 that $X_{Ca_2Fe_3Si_3O_{12}(OH)}$ decreases with decreasing values of f_{O_2}. Note that stoichiometric epidote may coexist with quartz, magnetite, and an aqueous phase only if f_{O_2} is close to that corresponding to the hematite–magnetite buffer and $a_{Ca^{++}}/a_{H^+}{}^2$ is near that required for quartz–hematite–andradite equilibrium. At 500°C and 1 kb, epidote solid solutions are stable if $\log f_{O_2} \geqslant -25.3$ (fig. 13). At values

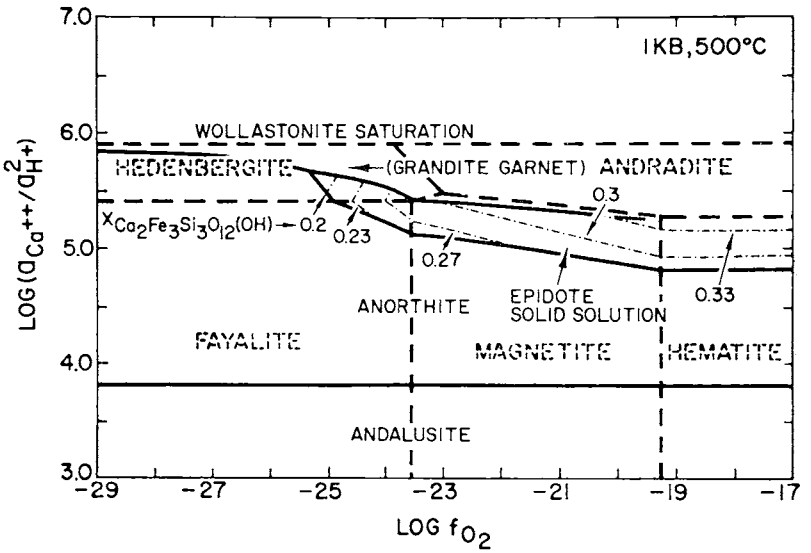

Fig. 13. Phase relations in the system CaO–FeO–Fe_2O_3–Al_2O_3–SiO_2–HCl–H_2O in the presence of quartz and other minerals in the subsystem CaO–FeO–Fe_2O_3–SiO_2 (indicated by the dashed labels) as a function of $\log f_{O_2}$ and $\log (a_{Ca^{++}}/a_{H^+}{}^2)$ in the aqueous phase at 500°C, 1 kb and $a_{H_2O} \approx 1$ (see caption of fig. 12).

of f_{O_2} less than this, epidote solid solutions in the presence of quartz and an aqueous phase are metastable relative to coexisting anorthite, hedenbergite, garnet, and an aqueous solution.

Equilibrium temperatures for reactions among minerals in the system CaO–Al_2O_3–SiO_2–H_2O as a function of $a_{CaAl_2Si_2O_8}$ in plagioclase.—Univariant and divariant equilibrium among stoichiometric minerals (represented by ψ_i, where $i = 1, 2, \ldots \hat{\imath}$) in the system CaO–Al_2O_3–SiO_3–H_2O in the presence of plagioclase and an aqueous phase can be expressed by writing a general reaction of the form

$$\sum_{i=1}^{\hat{\imath}} \hat{n}_{i,r}\,\psi_i + \hat{n}_{CaAl_2Si_2O_8,r}\,CaAl_2Si_2O_8 + \hat{n}_{H_2O,r}\,H_2O = 0 \qquad (24)$$

where $\hat{n}_{i,r}$ and $\hat{n}_{H_2O,r}$ stand for the reaction coefficients of the ith stoichiometric mineral and H_2O in the rth reaction, which are positive for prod-

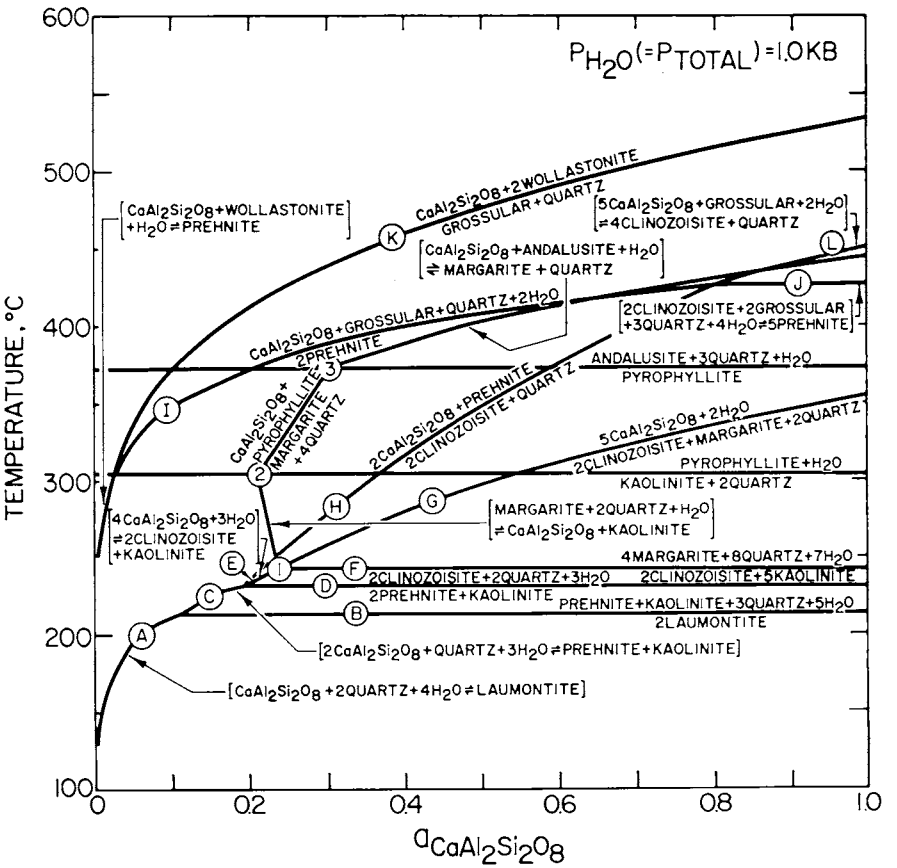

Fig. 14. Phase relations in the system CaO–Na_2O–Al_2O_3–SiO_2–H_2O at 1 kb in the presence of quartz and an aqueous solution in which $a_{H_2O} \approx 1$ as a function of temperature and $a_{CaAl_2Si_2O_8}$ in plagioclase. The numbered symbols designate isobaric invariant points, but the lettered symbols refer to the curves labeled with the same letters in figure 20.

ucts and negative for reactants, and $\hat{n}_{CaAl_2Si_2O_8,r}$ refers to the corresponding reaction coefficient of the anorthite component of plagioclase in the reaction. The law of mass action for reaction (24) can be written for $a_{H_2O} = 1$ as

$$(a_{CaAl_2Si_2O_8,})^{(\hat{n}_{CaAl_2Si_2O_8,r})} = K_r \tag{25}$$

where K_r represents the equilibrium constant for the subscripted statement of reaction (24). The logarithmic partial derivatives of eq (25) with respect to temperature at constant pressure, and pressure at constant temperature can be written as

$$\left(\frac{\partial \ln a_{CaAl_2Si_2O_8}}{\partial T}\right)_P = \frac{\Delta H^\circ_r}{RT^2 \hat{n}_{CaAl_2Si_2O_8,r}} \tag{26}$$

and

$$\left(\frac{\partial \ln a_{CaAl_2Si_2O_8}}{\partial P}\right)_T = -\frac{\Delta V^\circ_r}{RT \hat{n}_{CaAl_2Si_2O_8,r}} \tag{27}$$

respectively, where ΔH°_r and ΔV°_r stand for the standard molal enthalpy and volume change for the rth statement of reaction (24).

It follows from eq (26) that the temperature dependence of the activity of the anorthite component of plagioclase coexisting with stoichiometric minerals and an aqueous phase in the system CaO–Na_2O–Al_2O_3–SiO_2–HCl–H_2O is controlled by ΔH°_r for the various reactions involving plagioclase in figures 14 and 15. It can be deduced from the curves in these figures that if $\hat{n}_{CaAl_2Si_2O_8}$ is negative for all these reactions, ΔH°_r is also negative, except in the case of the reaction represented by the isobaric univariant curve connecting invariant points 1 and 2 in figure 14. The latter reaction can be written as

$$\underset{(kaolinite)}{CaAl_2Si_2O_8} + \underset{}{Al_2Si_2O_5(OH)_4} \rightleftharpoons \underset{(margarite)}{CaAl_2(Al_2Si_2O_{10})(OH)_2} + \underset{(quartz)}{2\,SiO_2} + H_2O \tag{28}$$

The values of ΔH°_r for all the other reactions written with $CaAl_2Si_2O_8$ on the left range from ~ -4 to ~ -50 kcal mole^{-1}, and ΔV°_r varies from ~ -5 to < -100 cm^3 mole^{-1}. Hence $a_{CaAl_2Si_2O_8}$ in the plagioclase involved in these reactions increases with increasing temperature at constant pressure but decreases with increasing pressure at constant temperature.

The phase relations depicted in figures 14 and 15 are shown in figures 16 and 17 as a function of temperature and $a_{Ca^{++}}/a_{H^+}{}^2$ in the coexisting aqueous phase. The "railroad" curves in these figures represent isopleths of $a_{CaAl_2Si_2O_8}$ in plagioclase. It can be deduced from figures 14 through 17 that clinozoisite, plagioclase, quartz and an aqueous solution are compatible over a wide range of temperature and $a_{CaAl_2Si_2O_8}$. Note that increasing pressure at constant $a_{CaAl_2Si_2O_8}$ increases the equilibrium temperature but decreases $a_{Ca^{++}}/a_{H^+}{}^2$ in the aqueous phase coexisting with plagioclase, clinozoisite, and quartz. For example, clinozoisite, quartz, and an aqueous solution are compatible with plagioclase in which $a_{CaAl_2Si_2O_8} = 0.5$ between 295° and 350°C, where $\log (a_{Ca^{++}}/a_{H^+}{}^2) = 7.6$ to 7.8 at 1 kb (figs. 14

and 16). However, at 5 kb the assemblage is stable between 425° and 530°C at log $(a_{Ca^{++}}/a_{H^+}{}^2) = 6.5$ to 7.2 (figs. 15 and 17).

Petrologic observations of metamorphosed pelites in the central Swiss Alps by Frey and Orville (1974) indicate that the $CaAl_2Si_2O_8$ content of plagioclase coexisting with margarite in the absence of clinozoisite is nearly constant with increasing metamorphic grade. However, in some rocks the transition from greenschist to amphibolite facies is accompanied by unusually high mole fractions of $CaAl_2Si_2O_8$ in plagioclase assoicated with margarite. These petrologic observations are in close agreement with the calculated phase relations shown in figures 14 and 16. For example, equilibrium among margarite, plagioclase, and quartz in the presence of an aqueous solution and kaolinite or pyrophyllite can be represented by reaction (28) and

$$\underset{(pyrophyllite)}{CaAl_2Si_2O_8 + Al_2Si_4O_{10}(OH)_2} = \underset{(margarite)}{CaAl_2(Al_2Si_2O_{10})\,(OH)_2} + \underset{(quartz)}{4\,SiO_2} \qquad (29)$$

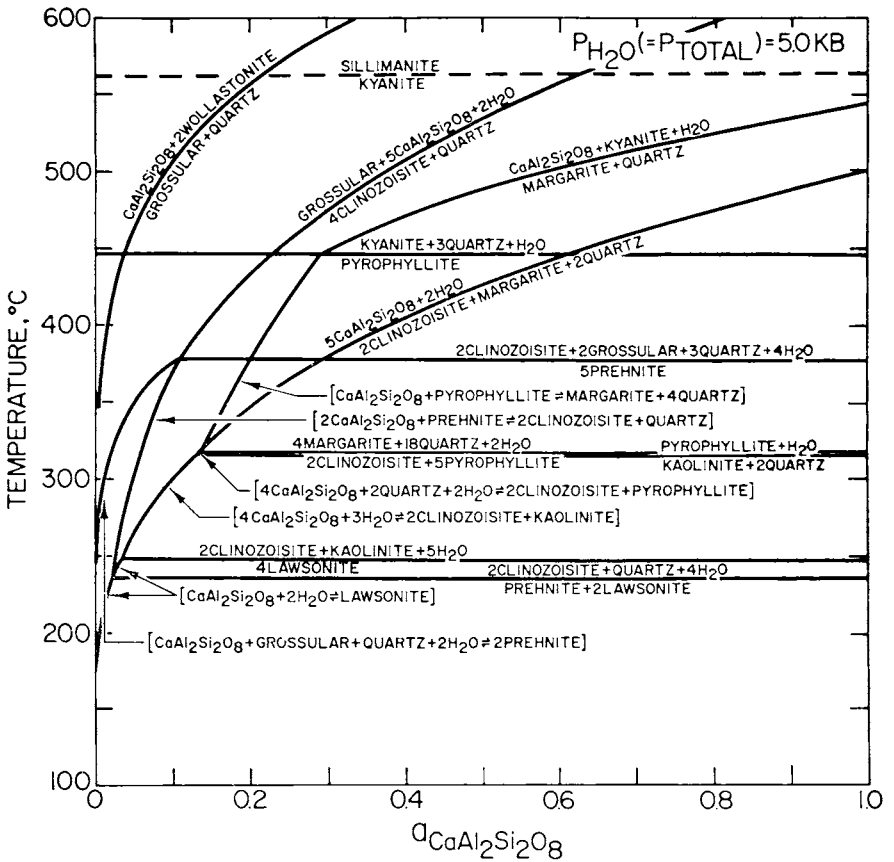

Fig. 15. Phase relations in the system CaO–Na_2O–Al_2O_3–SiO_2–H_2O at 5 kb in the presence of quartz and an aqueous solution in which $a_{H_2O} \approx 1$ as a function of temperature and $a_{CaAl_2Si_2O_8}$ in plagioclase.

The curves connecting invariant points 1, 2, and 3 in figure 14 represent the equilibrium constants for these reactions, which vary only slightly as a function of temperature. As a consequence, the variation of $a_{CaAl_2Si_2O_8}$ in plagioclase coexisting with margarite, quartz, and an aqueous phase in the presence of kaolinite or pyrophyllite between ~ 240° and 370°C at 1 kb is restricted to values between ~ 0.2 and 0.3. However, it can be seen in figure 14 that at higher temperatures where pyrophyllite is not stable at 1 kb, $a_{CaAl_2Si_2O_8}$ increases dramatically with increasing temperature in plagioclase coexisting with margarite, quartz, andalusite, and an aqueous phase, which can be expressed as

$$\underset{(andalusite)}{CaAl_2Si_2O_8} + Al_2SiO_5 + H_2O = \underset{(margarite)}{CaAl_2(Al_2Si_2O_{10})(OH)_2} + \underset{(quartz)}{SiO_2} \quad (30)$$

COMPOSITIONAL CONSTRAINTS IMPOSED BY COEXISTING EPIDOTE, GARNET, AND PLAGIOCLASE SOLID SOLUTIONS IN METAMORPHIC PROCESSES

Petrologic observations of metamorphic rocks containing plagioclase and epidote solid solutions from the Hohe Tauern area of Austria by Hörmann and Raith (1973) and Morteani and Raase (1974) indicate that $X_{CaAl_2Si_2O_8}$ in the plagioclase is correlative with local compositional variation in the coexisting epidote solid solutions. Their observations

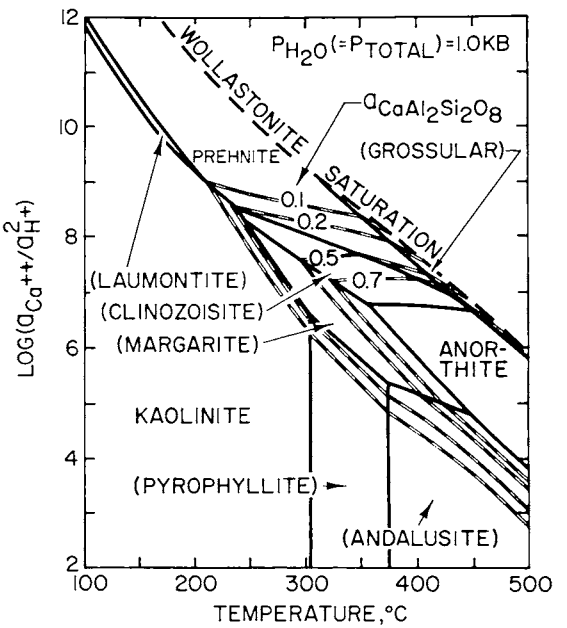

Fig. 16. Phase relations in the system $CaO–Na_2O–Al_2O_3–SiO_2–HCl–H_2O$ at 1 kb in the presence of quartz and an aqueous solution in which $a_{H_2O} \approx 1$ as a function of temperature and log ($a_{Ca^{++}}/a_{H^+}^2$) in the aqueous phase. The dashed curve designates saturation of the aqueous phase with respect to wollastonite, but the "railroad" curves represent isopleths of the activity of the anorthite component of plagioclase.

indicate also that $X_{CaAl_2Si_2O_8}$ is greater in plagioclase coexisting with clinozoisite-rich epidote solid solutions than that in plagioclase associated with epidote-rich solid solutions in adjacent strata. These observations can be correlated with fluid and mineral compositions by taking explicit account of the thermodynamic behavior of epidote and plagioclase solid solutions at high pressures and temperatures.

Phase relations among epidote and plagioclase solid solutions at 500°C and 5 kb are shown in figure 18 as a function of $a_{Ca^{++}}/a_{H^+}{}^2$ and $a_{Fe^{+++}}/a_{H^+}{}^3$ in the coexisting aqueous solution. Isopleths corresponding to constant activity of $CaAl_2Si_2O_8$ in plagioclase are shown for $a_{CaAl_2Si_2O_8} =$ 0.3, 0.5, and 0.7. None is shown for unit activity of $CaAl_2Si_2O_8$ because stoichiometric anorthite is not stable in this system at 500°C and 5 kb. Note that $a_{Ca^{++}}/a_{H^+}{}^2$ in the aqueous phase coexisting with epidote and plagioclase solid solutions decreases with increasing $a_{Fe^{+++}}/a_{H^+}{}^3$ at constant $a_{CaAl_2Si_2O_8}$ in response to increasing substitution of Fe^{+++} for Al^{+++} in the epidote solid solution. It can be seen in figure 18 that epidote solid solutions in which $X_{Ca_2Fe_3Si_3O_{12}(OH)} \lesssim 0.03$ may coexist with plagioclase, quartz, and an aqueous phase over a wide range of $a_{CaAl_2Si_2O_8}$, $a_{Ca^{++}}/a_{H^+}{}^2$, and $a_{Fe^{+++}}/a_{H^+}{}^3$. In contrast, this range is restricted severely if $X_{Ca_2Fe_3Si_3O_{12}(OH)}$ in the epidote solid solution is $\geqslant 0.27$. Note also that at constant pressure,

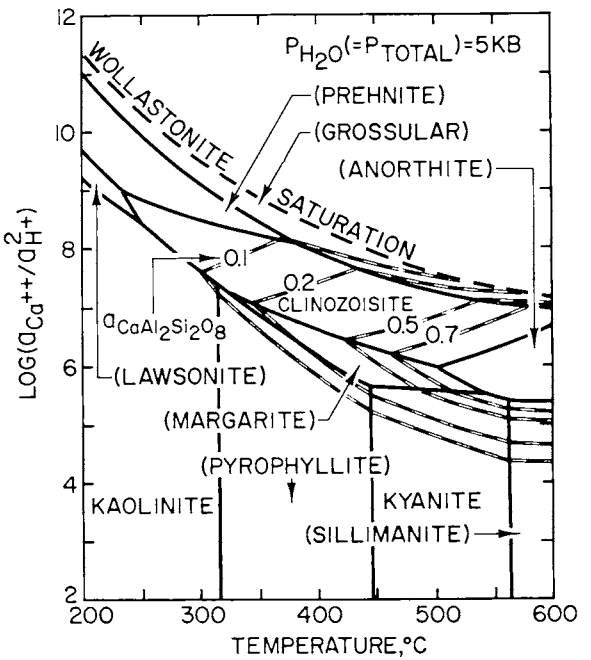

Fig. 17. Phase relations in the system CaO–Na_2O–Al_2O_3–SiO_2–HCl–H_2O at 5 kb in the presence of quartz and an aqueous solution in which $a_{H_2O} \approx 1$ as a function of temperature and log ($a_{Ca^{++}}/a_{H^+}{}^2$) in the aqueous phase (see caption of fig. 16).

temperature, and $a_{Ca^{++}}/a_{H^+}^2$, $X_{Ca_2Fe_3Si_3O_{12}(OH)}$ increases, but $a_{CaAl_2Si_2O_8}$ decreases with increasing $a_{Fe^{+++}}/a_{H^+}^3$ in the aqueous phase.

Compositional constraints imposed on the aqueous phase by the compatibility of plagioclase and epidote solid solutions at 500°C and 5 kb are shown in figure 19, where a number of the stability fields depicted in figure 18 are plotted as a function of $a_{CaAl_2Si_2O_8}$ and $X_{Ca_2Fe_3Si_3O_{12}(OH)}$. It can be seen that $a_{CaAl_2Si_2O_8}$ in plagioclase coexisting with epidote solid solutions decreases dramatically with increasing Fe^{+++} substitution for Al^{+++} in the epidote solid solutions. Note that stoichiometric clinozoisite, quartz, and an aqueous phase may coexist with plagioclase in which $0.375 \leqslant a_{CaAl_2Si_2O_8} \leqslant 0.99$, but stoichiometric epidote, quartz, plagioclase, and an aqueous solution are restricted to $a_{CaAl_2Si_2O_8} \approx 0.11$ to 0.13.

The relative stabilities of plagioclase, stoichiometric calcium–aluminum silicates, and garnet and epidote solid solutions are shown in figures 20 and 21 as a function of $a_{CaAl_2Si_2O_8}$, temperature, and pressure along a "typical" geothermal profile with a gradient of 100°C kb^{-1} (≈ 30°C km^{-1}). The lettered symbols in figure 20 represent the reactions and

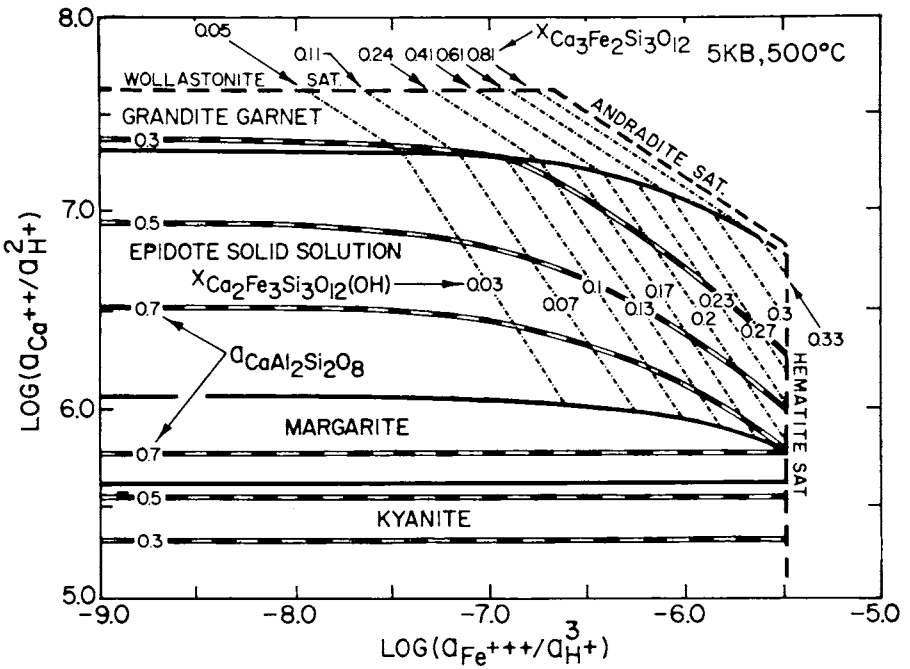

Fig. 18. Phase relations in the system CaO–Na_2O–Fe_2O_3–Al_2O_3–SiO_2–HCl–H_2O in the presence of quartz and an aqueous solution in which $a_{H_2O} \approx 1$ at 5 kb and 500°C as a function of log ($a_{Ca^{++}}/a_{H^+}^2$) and log ($a_{Fe^{+++}}/a_{H^+}^3$) in the aqueous phase. The long-dash curves represent saturation of the fluid phase with respect to wollastonite, andradite, or hematite, but the short-dash curve corresponds to an extrapolation of the stability field boundary separating epidote and grandite solid solutions to $X_{Ca_2Fe_3Si_3O_{12}(OH)} > 0.33$ (see text). The dot-dash curves denote compositional isopleths for epidote and grandite garnet solid solutions, but the "railroad" curves designate activities of the anorthite component of plagioclase.

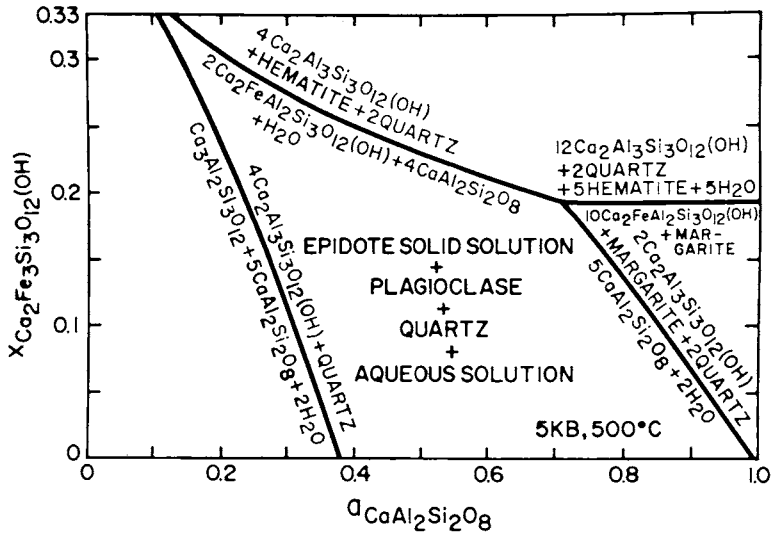

Fig. 19. Activity/composition relations for coexisting epidote and plagioclase solid solutions, quartz, and an aqueous phase in which $a_{H_2O} \approx 1$ at 500°C and 5 kb.

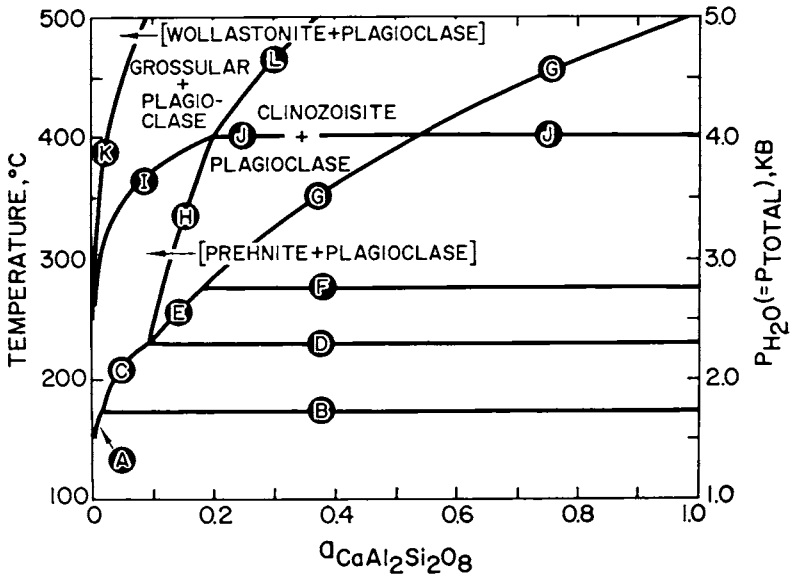

Fig. 20. Phase relations in the system $CaO–Na_2O–Al_2O_3–SiO_2–H_2O$ along a geotherm with a 100°C kb^{-1} gradient in the presence of quartz and an aqueous solution in which $a_{H_2O} \approx 1$ as a function of temperature, pressure, and $a_{CaAl_2Si_2O_8}$ in plagioclase. The letters designate corresponding reactions in figure 14.

curves similarly labeled in figure 14, but the stability field boundaries in figure 21 were generated from the laws of mass action for

$$4\,Ca_2Al_3Si_3O_{12}(OH) + Fe_2O_3 + 2\,SiO_2 \rightleftharpoons 2\,Ca_2FeAl_2Si_3O_{12}(OH) + 4\,CaAl_2Si_2O_8 + H_2O \quad (31)$$

(*hematite*) (*quartz*)

and

$$4\,Ca_2Al_3Si_3O_{12}(OH) + SiO_2 \rightleftharpoons Ca_3Al_2Si_3O_{12} + 5\,CaAl_2Si_2O_8 + 2\,H_2O \quad (32)$$

(*quartz*)

It can be seen in figures 20 and 21 that increasing pressure and temperature along the geothermal profile represented by the ordinate increases dramatically the range of $a_{CaAl_2Si_2O_8}$ in plagioclase coexisting with clinozoisite-bearing assemblages. In contrast, plagioclase coexisting with epidote, quartz, and an aqueous phase (fig. 21) is constrained to a narrow range of $a_{CaAl_2Si_2O_8}$ ($\leqslant 0.02$). Note also in figure 22 that $a_{CaAl_2Si_2O_8}$ in plagioclase coexisting with epidote at 5 kb must be < 0.13, but for clinozoisite-bearing assemblages, $a_{CaAl_2Si_2O_8}$ is constrained to be > 0.11 (fig. 20). It follows from these observations that the temperature dependence of the mole fraction of $CaAl_2Si_2O_8$ in plagioclase is highly sensitive to the composition of coexisting epidote solid solutions.

Various observations by Miyashiro and Seki (1958), Holdaway (1965), Ernst and others (1970), Ghent and DeVries (1972), Rambaldi (1973), Hörmann and Raith (1973), Raith (1976), and others indicate a general tendency for $X_{Ca_2Fe_3Si_3O_{12}(OH)}$ in epidote solid solutions to decrease with increasing metamorphic grade. Changes in bulk composition and the

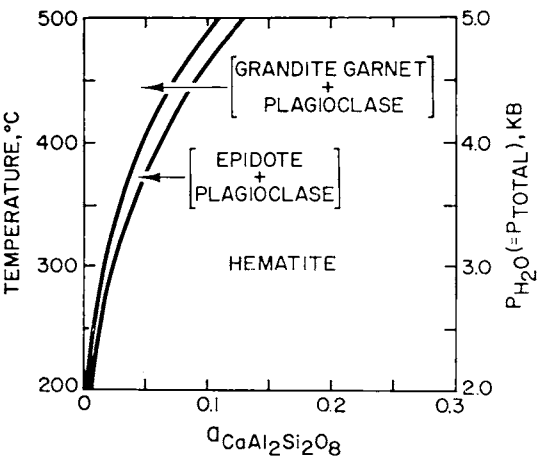

Fig. 21. Phase relations in the system CaO–Na_2O–Fe_2O_3–Al_2O_3–SiO_2–H_2O along a geotherm with a 100°C kb^{-1} gradient in the presence of quartz and an aqueous solution in which $a_{H_2O} \approx 1$ as a function of temperature, pressure, and $a_{CaAl_2Si_2O_8}$ in plagioclase.

fugacity of oxygen appear to be partly responsible for these observations, which are consistent with the phase relations shown in figures 9, 10, and 22. For example, inspection of figures 9 and 10 indicates that $X_{Ca_2Fe_3Si_3O_{12}(OH)}$ in epidote solid solutions coexisting with margarite, anorthite, quartz, hematite, and an aqueous phase decreases from a value of 0.22 at 1 kb and 410°C to ~ 0.18 at 5 kb and 525°C. Similarly, it can be seen in figure 22 that $X_{Ca_2Fe_3Si_3O_{12}(OH)}$ in epidote solid solutions decreases as $a_{CaAl_2Si_2O_8}$ increases in coexisting plagioclase solid solutions which equilibrate consecutively with kaolinite, pyrophyllite, and margarite, with increasing temperature at constant pressure.

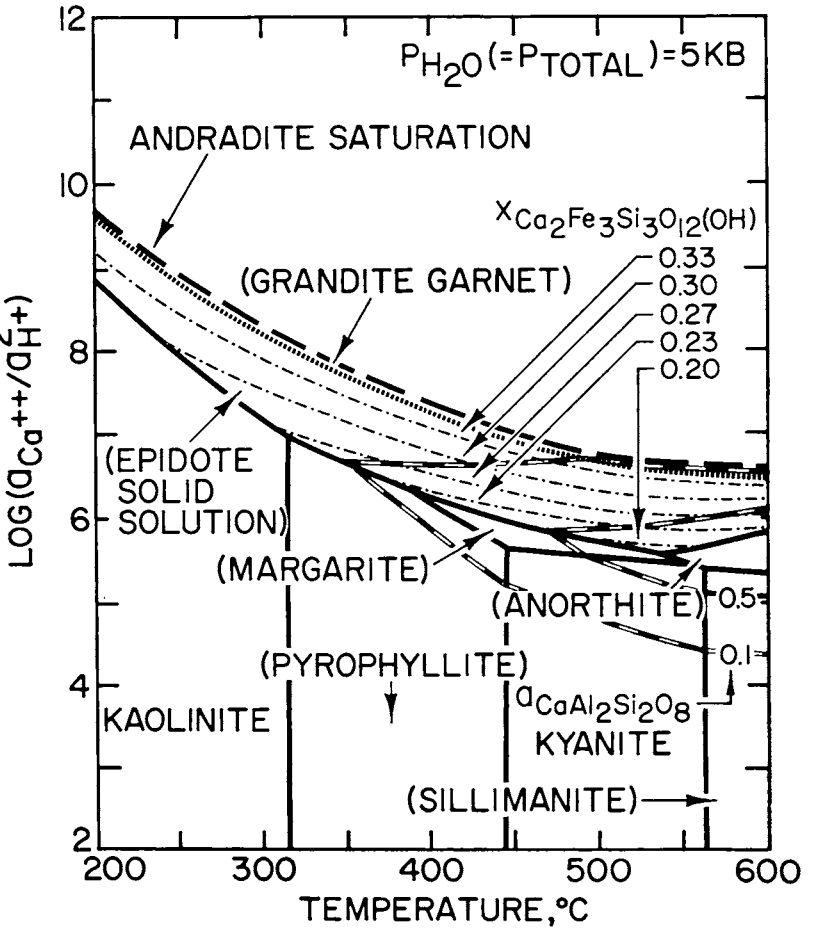

Fig. 22. Phase relations in the system $CaO–Na_2O–Fe_2O_3–Al_2O_3–SiO_2–HCl–H_2O$ at 5 kb in the presence of quartz, hematite, and an aqueous solution in which $a_{H_2O} \approx 1$ as a function of temperature and log ($a_{Ca^{++}}/a_{H^+}^2$) in the aqueous phase. The dashed curve represents saturation of the fluid phase with respect to andradite, but the dotted curve corresponds to an extrapolation of the stability field boundary separating epidote and grandite garnet solid solutions to $X_{Ca_2Fe_3Si_3O_{12}(OH)} > 0.33$ (see text). The "railroad" curves denote isopleths of $a_{CaAl_2Si_2O_8}$ in plagioclase.

The consequences of increasing X_{CO_2} in the fluid phase on the mineral compositions and compatibilities discussed above are shown in figures 23 and 24. Isopleths of $a_{CaAl_2Si_2O_8} = 0.5$ and 0.25 in plagioclase are shown in figure 23, but those in figure 24 correspond to $a_{CaAl_2Si_2O_8} = 1.0$, 0.95, 0.9, 0.7, and 0.5. It can be seen in these figures that the compositions of coexisting epidote and plagioclase solid solutions are sensitive functions of both X_{CO_2} and $a_{Fe^{+++}}/(\sigma_{Fe^{+++}} a_{H^+}{}^3)$ in the fluid phase.

The symbols shown in figures 23 and 24 represent average mineral compositions for coexisting epidote and plagioclase solid solutions reported by Rambaldi (1973) and Ghent and DeVries (1972) for staurolite-grade metamorphic rocks, which were plotted assuming $a_{CaAl_2Si_2O_8} \approx$

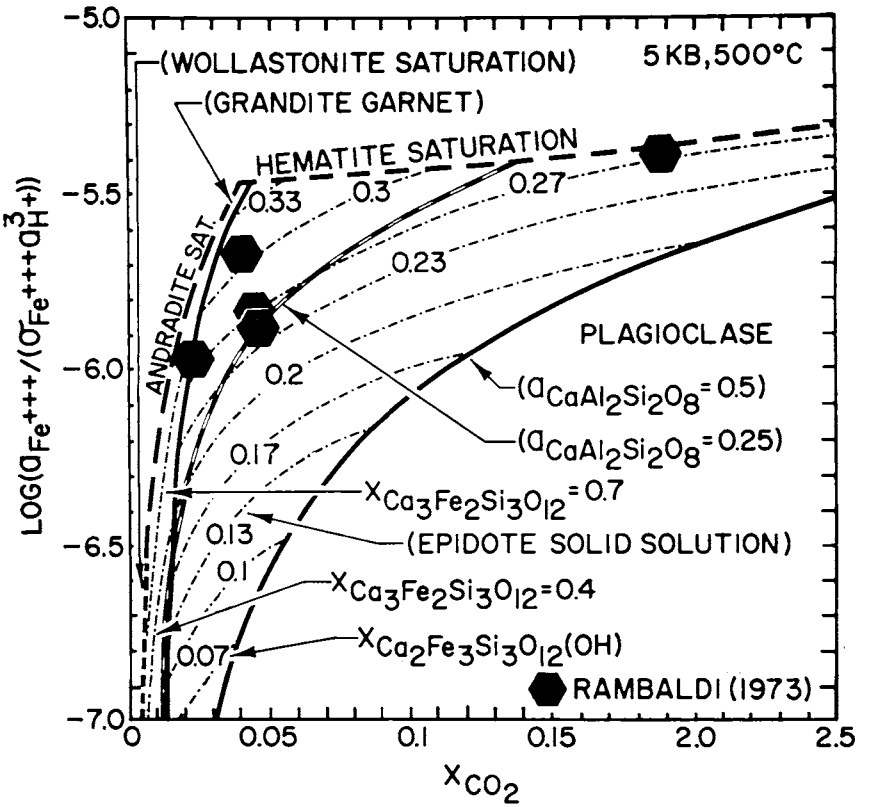

Fig. 23. Phase relations in the system CaO–Na_2O–Fe_2O_3–Al_2O_3–SiO_2–HCl–H_2O–CO_2 in the presence of quartz and calcite as a function of log $(a_{Fe^{+++}}/(\sigma_{Fe^{+++}} a_{H^+}{}^3))$ and X_{CO_2} in the fluid phase at 500°C and 5 kb. The long-dash curve represents saturation of the fluid phase with respect to hematite, but the short-dash curve corresponds to an extrapolation of the stability field boundary separating epidote and grandite garnet solid solutions to $X_{Ca_2Fe_3Si_3O_{12}(OH)} > 0.33$ (see text). The "railroad" curves represent constant activities of the anorthite component of plagioclase and the dot-dash curves denote compositional isopleths for epidote and grandite garnet solid solutions. The symbols represent analytical compositions of coexisting epidote and plagioclase solid solutions (see text and caption of fig. 11).

$X_{CaAl_2Si_2O_8}$. In all cases the symbols represent highly zoned epidote and plagioclase solid solutions. It can be deduced from figures 23 and 24 that minor fluctuations in fluid composition under isobaric and/or isothermal conditions can account for the complex zoning observed in these minerals. For example, compositional variation amounting to ± 5 mole percent of either $Ca_2Fe_3Si_3O_{12}(OH)$ or $CaAl_2Si_2O_8$ in coexisting epidote and plagioclase solid solutions may result from changes in X_{CO_2} and log $(a_{Fe^{+++}}/(\sigma_{Fe^{+++}}\, a_{H^+}{}^3))$ of only ± 0.02 and ± 0.3, respectively.

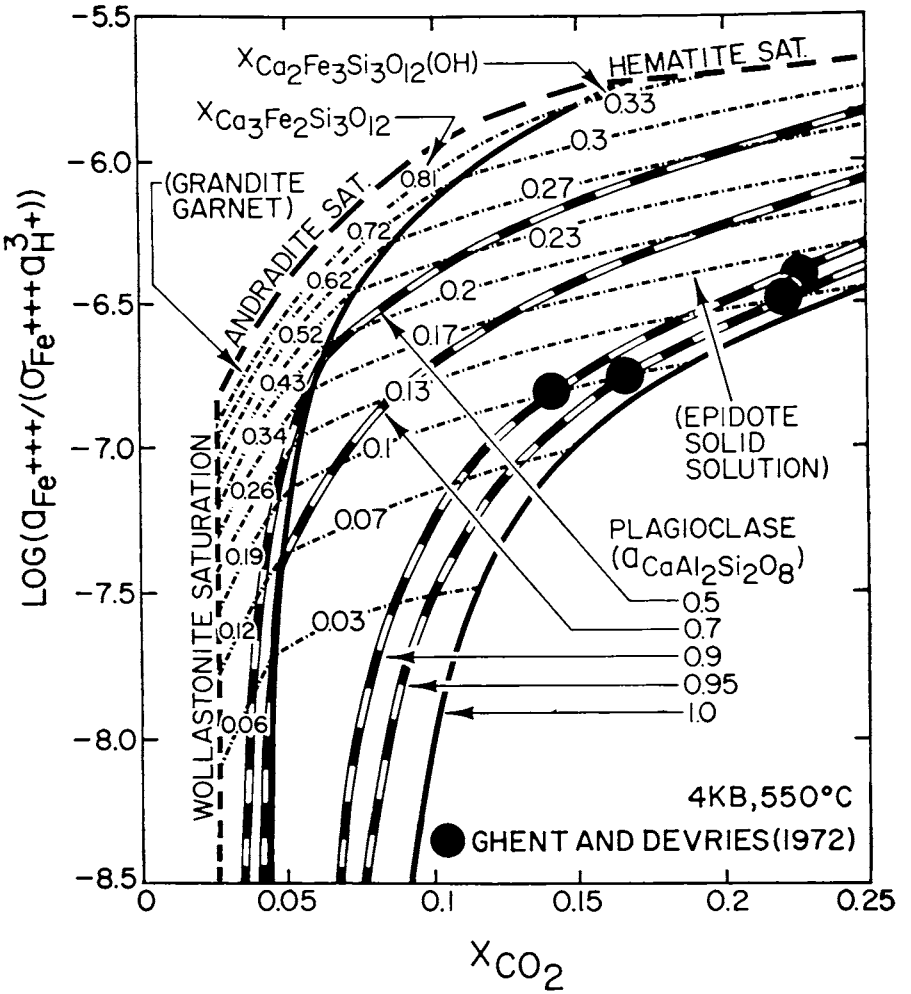

Fig. 24. Phase relations in the system $CaO–Na_2O–Fe_2O_3–Al_2O_3–SiO_2–H_2O–HCl–CO_2$ in the presence of quartz and calcite as a function of log $(a_{Fe^{+++}}/(\sigma_{Fe^{+++}}a_{H^+}{}^3))$ and X_{CO_2} in the fluid phase at 550°C and 4 kb (see text and captions of figs. 11 and 23).

CORRELATION OF MINERAL AND FLUID COMPOSITIONS IN GEOTHERMAL RESERVOIRS

Exploitation of active geothermal systems permits correlation of the compositions of hydrothermal solutions and associated mineral assemblages with measured pressures and temperatures. Deep drill holes in such systems near the Circum-Pacific margin commonly encounter epidote solid solutions coexisting with albite and K-feldspar in hydrothermally altered Quaternary to Recent volcanic and sedimentary rocks. It can be shown that for the most part calculated compositions of the aqueous phase coexisting with these minerals compare favorably with published chemical analyses of reservoir fluids in geothermal systems (see below).

Epidote, albite, K-feldspar, K-mica, and quartz.—This mineral assemblage is common in a number of active geothermal systems near the Circum-Pacific margin, including those at Wairakei, New Zealand (Steiner, 1953, 1968), Otake, Japan (Hayashi and Yamasaki, 1976), and Pauzhetka, USSR (Noboko, 1970, 1976). These systems occur in Quaternary to Recent volcanic rocks consisting of rhyolitic, andesitic, and dacitic flows, tuffs, and ignimbrites associated with Pacific margin tectonism. Measured temperatures are $\lesssim 300°C$, and the solute of the reservoir fluids consists primarily of NaCl and KCl with ionic strengths of ~ 0.1 or less. Carbon dioxide is a minor component of the fluids.

Equilibrium among epidote, alkali feldspar, and mica solid solutions in the presence of quartz and an aqueous phase can be represented by writing

$$6\,KAlSi_3O_8 + 3\,NaAlSi_3O_8 + 4\,Ca^{++} + 2\,H_2O \rightleftharpoons 2\,Ca_2Al_3Si_3O_{12}(OH) + KAl_2(AlSi_3O_{10})(OH)_2 + 18\,SiO_2 + 3\,Na^{+} + 5\,K^{+} \qquad (33)$$

(*quartz*)

for which the law of mass action appears as

$$\left(\frac{(a_{Ca_2Al_3Si_3O_{12}(OH)})^2(a_{KAl_2(AlSi_3O_{10})(OH)_2})}{(a_{KAlSi_3O_8})^6(a_{NaAlSi_3O_8})^3}\right)\left(\frac{(a_{Na^+})^3(a_{K^+})^5}{(a_{Ca^{++}})^4(a_{H_2O})^2}\right) = K \qquad (34)$$

where K stands for the equilibrium constant for reaction (33). If the activities of $NaAlSi_3O_8$, $KAlSi_3O_8$, $KAl_2(AlSi_3O_{10})(OH)_2$, and H_2O are set to unity in eq (34), the logarithm of the expression can be written as

$$\log K - 2\log a_{Ca_2Al_3Si_3O_{12}(OH)} = \log (a_{Na^+}{}^3\, a_{K^+}{}^5\, a_{Ca^{++}}{}^{-4}) \qquad (35)$$

which is represented by the curves and symbols in figure 25. The symbols shown in the figure represent values of the right side of eq (35) computed from published analyses of reservoir fluids using activity coefficients and dissociation constants taken from Helgeson (1969), but the curves were generated from thermodynamic equations and data given by Helgeson and Kirkham (1974a), Helgeson, Kirkham, and Flowers (1981), Helgeson and others (1978), and Bird and Helgeson (1980), which provide for equilibrium order/disorder in K-feldspar, albite, and epidote solid solutions.

The symbols for Wairakei represent composite values for wells producing from the Waiora fault zone, but the other symbols correspond to individual analyses.

It can be seen in figure 25 that the symbols and curves are in close agreement with one another. Although the slight compositional variation exhibited by micas and feldspars in geothermal systems has little effect on this observation, metastable disorder in either albite or K-feldspar may increase ($a_{Na^+}{}^3\ a_{K^+}{}^5\ a_{Ca^{++}}{}^{-4}$) by as much as several orders of magnitude. It thus appears from the close correlation of the calculated and measured temperatures and fluid compositions in figure 25 that the feldspars in the geothermal systems considered in the figure are almost completely ordered, and that $X_{Ca_2Fe_3Si_3O_{12}(OH)} \lesssim 0.28$ in the coexisting epidote solid solutions. In contrast, the authigenic K-feldspar in the Salton Sea geothermal system is almost completely disordered (see below).

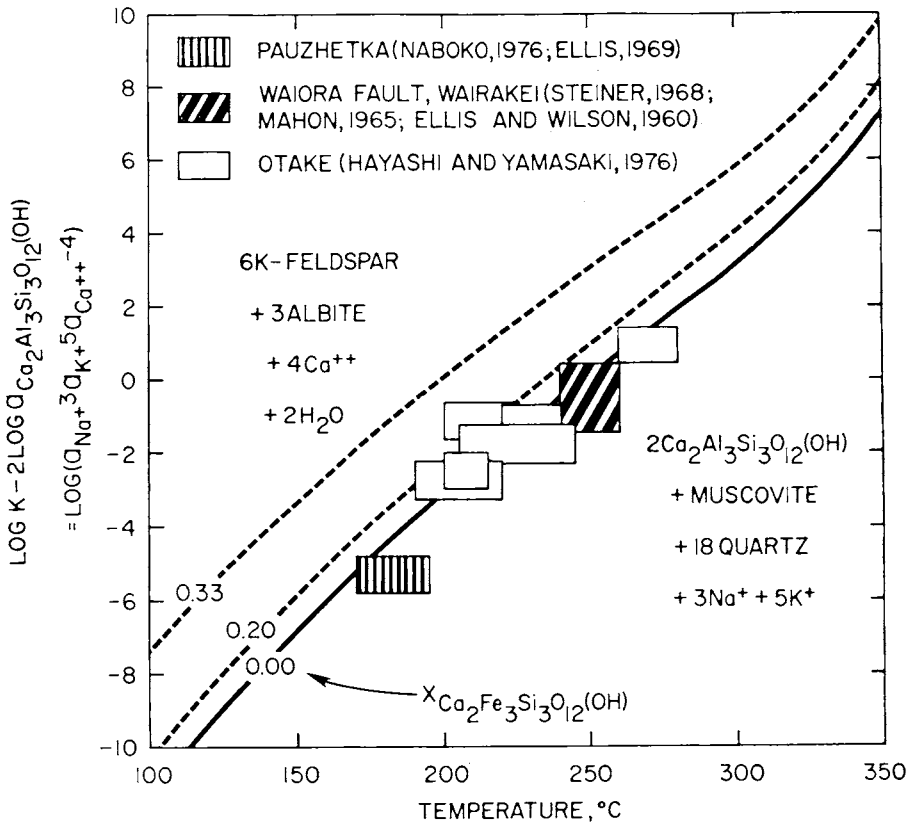

Fig. 25. Activity-temperature diagram for an aqueous phase coexisting with albite, K-feldspar, muscovite, quartz, and epidote solid solutions at pressures corresponding to those along the liquid-vapor equilibrium curve for H_2O. The solid and dashed curves represent compositional isopleths for epidote solid solutions generated from equations given in the text, but the symbols represent values of log ($a_{Na^+}{}^3\ a_{K^+}{}^5\ a_{Ca^{++}}{}^{-4}$) computed from analyses of geothermal reservoir fluids reported to be coexisting with the above assemblage — see text.

Epidote, K-feldspar, K-mica, calcite, and quartz.—This mineral assemblage occurs at depths ranging from ~ 0.6 to 1.1 km in the arkosic sands of the Colorado River delta in the Salton Sea geothermal system of southern California (Helgeson, 1967, 1968; Keith, Muffler, and Cremer, 1968; Muffler and White, 1969; Kendall, ms; McDowell and McCurry, 1977). X-ray and petrographic analyses of drill core and cuttings taken from this depth interval indicate that the relative abundances of calcite and K-mica decrease, but those of epidote and K-feldspar increase with increasing depth and temperature. The measured temperatures range from ~ 250° to 325°C, and the aqueous phase associated with this mineralization contains large concentrations of NaCl, $CaCl_2$, and KCl with a stoichiometric ionic strength > 5.

It has been shown (McDowell and Elders, 1978; D. McDowell, 1978, written commun.; Bird and Norton, 1979) that $a_{KAl_2(AlSi_3O_{10})(OH)_2} \approx 0.6$ in the coarse-grained authigenic K-mica solid solution recovered from depths of ~ 0.8 to 1.0 km in the Elmore no. 1 well in the Salton Sea geothermal system, and that the coexisting K-feldspar corresponds to sanidine. The epidote solid solution in the assemblage is compositionally zoned with $X_{Ca_2Fe_3Si_3O_{12}(OH)}$ ranging from ~ 0.15 to 0.25 (McDowell and McCurry, 1977). Other authigenic phases include albite, anhydrite, pyrite, chlorite, quartz, and calcite. Representing equilibrium among these various minerals and the aqueous solution with hydrolysis reactions makes it possible to calculate $a_{Ca^{++}}/a_{H^+}{}^2$, a_{Na^+}/a_{H^+}, a_{K^+}/a_{H^+}, $a_{Fe^{++}}/a_{H^+}{}^2$, $a_{Al^{+++}}/a_{H^+}{}^3$, $a_{SiO_{2(aq)}}$, $a_{Fe^{+++}}/a_{H^+}{}^3$, $f_{O_{2(g)}}$, $f_{S_{2(g)}}$, and $f_{CO_{2(g)}}$ in the geothermal reservoir fluid by simultaneous evaluation of statements of the law of mass action for the reactions. Calculations of this kind (Bird and Norton, 1979) afford close approximation of the Salton Sea geothermal fluid composition reported by Helgeson (1967). For example, the compositional relations summarized above for epidote and K-mica solid solutions coexisting with sanidine, calcite, quartz, and an aqueous phase can be combined with the law of mass action for

$$3\,KAl_2(AlSi_3O_{10})(OH)_2 + 4\,CaCO_3 + 6\,SiO_2 \underset{(calcite)\quad(quartz)}{} \rightleftharpoons 2\,Ca_2Al_3Si_3O_{12}(OH) + 3\,KAlSi_3O_8 + 4\,CO_2 + 2\,H_2O \underset{(sanidine)}{} \tag{36}$$

to give (for unit activity of $KAlSi_3O_8$, $CaCO_3$, SiO_2, and H_2O)

$$\log f_{CO_2} = 0.25\,(\log K - 2\log a_{Ca_2Al_3Si_3O_{12}(OH)} + 3\log a_{KAl_2(AlSi_3O_{10})(OH)_2}) = 0.25\,(\log K - 2\log a_{Ca_2Al_3Si_3O_{12}(OH)} + 3\log (0.6)) \tag{37}$$

where K represents the equilibrium constant for reaction (36).

The curves in figure 26 were generated from eq (37) with $a_{KAl_2(AlSi_3O_{10})(OH)_2} = 0.6$ for $X_{Ca_2Fe_3Si_3O_{12}(OH)} = 0.0$, 0.2, and 0.33, but the symbols denote analytical fluid and mineral compositions in the Salton Sea geothermal system. The hexagons in figure 26 represent analytical compositions of coexisting epidote and K-mica solid solutions in the presence of

sanidine, calcite, and quartz, which are in close agreement with the hatched symbol representing the value of log $f_{CO_{2(g)}}$ in the geothermal reservoir reported by Helgeson (1967, 1968). It can be deduced from the curves shown in figure 26 that $a_{Ca^{++}}/a_{H^+}{}^2$ in the reservoir fluids decreases with increasing temperature at depths from ~ 0.8 to 1.0 km in the Salton Sea geothermal system.

CONCLUDING REMARKS

Although the compositions and compatibilities of coexisting minerals in the system K_2O–Na_2O–CaO–FeO–Fe_2O_3–Al_2O_3–SiO_2–H_2O–CO_2 are complicated functions of pressure, temperature, and fluid composition, they are commonly definitive with respect to the chemical conditions pre-

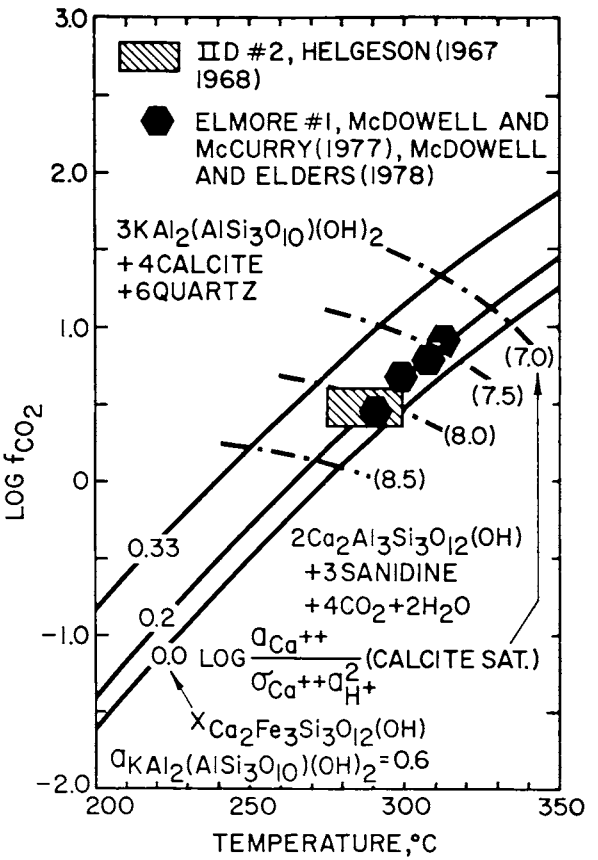

Fig. 26. Phase relations in the Salton Sea geothermal system as a function of temperature in the 11D no. 2 well (Helgeson, 1968). The curves represent compositional isopleths for epidote solid solutions generated from equations given in the text. The hexagons correspond to reported temperatures and compositions of epidote solid solutions coexisting with a K-mica solid solution ($a_{KAl_2(AlSi_3O_{10})(OH)_2} \approx 0.6$), sanidine, calcite, quartz, and the aqueous phase in the Salton Sea geothermal system. The hatched symbol represents the value of log f_{CO_2} reported by Helgeson (1967, 1968) for the production zone in the 11D no. 2 well (see text and caption of fig. 11).

vailing during metamorphic and geothermal processes in the Earth's crust. Analysis of the compositions of coexisting epidote and plagioclase solid solutions permits calculation of the thermodynamic consequences of metasomatism in metamorphic environments. Similarly, analysis of phase relations among epidote solid solutions and alkali feldspar mineral assemblages affords a means of predicting the compositions of geothermal reservoir fluids. Calculations of this kind can also be used to predict spatial changes in fluid composition from detailed petrographic descriptions and mineral analyses such as those presented by Kendall (ms), McDowell and McCurry (1977), Hoagland and Elders (1978), and others.

ACKNOWLEDGMENTS

The research reported above represents the second part of the senior author's Ph.D. dissertation at the University of California, Berkeley. We are indebted to Per Aagaard, Joan Delany, George Flowers, Connie Frisch, Ken Jackson, David Kirkham, William McKenzie, Heiko Oterdoom, Carol Schnake, Terri Bowers, John Walther, Mark Ghiorso, Barbara Rosenbaum, Joan Bossart, Mike Lee, Joachim Hampel, Derek Maskell, Debbie Montgomery, and others among our friends and colleagues at Berkeley for helpful suggestions, assistance, and encouragement during the course of this research. Various aspects of the project were supported by the National Science Foundation (NSF grants EAR 74-14280 and EAR 77-14492), the donors of the Petroleum Research Fund administered by the American Chemical Society (PRF grants 5356 AC2 and AC2C), the Miller Institute and Committee on Research at the University of California, Berkeley, the Lawrence Livermore and Lawrence Berkeley Laboratories of the University of California, and the Division of Physical Research of the U.S. Energy Research and Development Administration (ERDA Contracts UCB-ENG-4288 and W-7405-ENG-48). Finally, we would like to express our appreciation to M. J. Holdaway, B. J. Wood, C. Meyer, L. H. Cohen, D. L. Norton, W. M. Murphy, J. A. Trembly, and P. A. Witherspoon for reviewing the manuscript and offering many helpful suggestions for improvement.

REFERENCES

Aranovich, L. Ya., 1976, Phase correspondence in the system epidote–garnet (experimental data): Contr. Physico-Chem. Petrology, v. 6, p. 14-33.

Barth, T. F. W., 1952, Theoretical petrology: New York, John Wiley & Sons, 387 p.

Bird, D. K., and Helgeson, H. C., 1977, Prediction of the chemical characteristics of geothermal reservoir fluids from authigenic mineral assemblages [abs.]: Geol. Soc. America, Abs. with Programs, v. 9, p. 898-899.

———— 1980, Chemical interaction of aqueous solutions with epidote–feldspar mineral assemblages in geologic systems. I. Thermodynamic analysis of phase relations in the system CaO–FeO–Fe_2O_3–Al_2O_3–SiO_2–H_2O–CO_2: Am. Jour. Sci., v. 280, p. 907-941.

Bird, D. K., and Norton, D., 1979, Correlation of the spatial variations in the composition of geothermal reservoir fluids from petrological observations and thermodynamic calculations in the Salton Sea geothermal system [abs.]: Geol. Soc. America, Abs. with Programs, v. 11, no. 7, p. 388.

Brown, W. L., 1962, Peristerite unmixing in the plagioclases and metamorphic facies series: Norsk Geol. Tidsskr., v. 42, p. 354-382.

Browne, P. R. L., and Ellis, A. J., 1970, The Ohaki-Broadlands hydrothermal area, New Zealand: mineralogy and related geochemistry: Am. Jour. Sci., v. 269, p. 97-131.

Christie, O. H., 1959, Note on the equilibirum between plagioclase and epidote: Norsk Geol. Tidsskr., v. 39, p. 268-271.

———— 1962, Feldspar structure and the equilibrium between plagioclase and epidote (discussion): Am. Jour. Sci., v. 260, p. 149-153.

Crawford, M. L., 1966, Composition of plagioclase and associate minerals in some schists from Vermont, U.S.A., and south Westland, New Zealand, with inferences about the peristerite solvus: Contr. Mineralogy Petrology, v. 13, p. 269-294.

———— 1972, Plagioclase and other mineral equilibria in a contact metamorphic aureole: Contr. Mineralogy Petrology, v. 36, p. 293-314.

Delany, J. M., and Helgeson, H. C., 1978, Calculation of the thermodynamics of dehydration in subducting ocean crust to 100 kb and 800°C: Am. Jour. Sci., v. 278, p. 638-686.

de Waard, D., 1959, Anorthite content of plagioclase in basic and pelitic crystalline schists as related to metamorphic zoning in the Usu Masif, Timor: Am. Jour. Sci., v. 257, p. 562-574.

Eskola, P., 1920, The mineral facies of rocks, Norsk Geol. Tidsskr., v. 6, p. 143-194.

Ernst, W. G., Seki, Y., Onuki, H., and Gilbert, M. C., 1970, Comparative study of low grade metamorphism in the California Coast Ranges and the Outer Metamorphic Belt of Japan: Geol. Soc. America Mem. 124, 276 p.

Evans, B. W., 1964, Coexisting albite and oligoclase in some schists from New Zealand: Am. Mineralogist, v. 49, p. 173-179.

Flowers, G. C., 1979, Correction of Holloway's (1977) adaptation of the modified Redlich-Kwong equation of state to calculation of the fugacities of molecular species in supercritical fluids of geologic interest: Contr. Mineralogy Petrology, v. 69, p. 315-318.

Frey, M., and Orville, P. M., 1974, Plagioclase in margarite-bearing rocks: Am. Jour. Sci., v. 274, p. 31-47.

Fyfe, W. S., Turner, F. J., and Verhoogen, John, 1958, Metamorphic reactions and metamorphic facies: Geol. Soc. America Mem. 75, 253 p.

Garrison, J. R., Jr., 1978, Plagioclase compositions from metabasalts, southeastern Llano Uplift: plagioclase unmixing during amphibolite-grade metamorphism: Am. Mineralogist, v. 63, p. 143-149.

Ghent, E. D., and DeVries, C. D. S., 1972, Plagioclase–garnet–epidote equilibria in hornblende–plagioclase bearing rocks from the Esplanade Range, British Columbia: Canadian Jour. Earth Sci., v. 9, p. 618-635.

Goldsmith, J. R., 1978, Experimental plagioclase–zoisite phase relations [abs.]: Am. Geophys. Union Trans., v. 59, no. 4, p. 402.

Grove, T. L., 1976, Exsolution in metamorphic bytownite, *in* Wenk H.-R., ed., Electron Microscopy in Mineralogy: New York, Springer-Verlag, p. 266-270.

Haselton, H. T., Jr., and Westrum, E. F., Jr., 1980, Low temperature heat capacities of synthetic pyrope, grossular, and $pyrope_{60}grossular_{40}$: Geochim. et Cosmochim. Acta v. 44, p. 701-709.

Hayashi, M., and Yamasaki, T., 1976, Hydrothermal alteration of pyroxene andesites in the Otake geothermal area, Japan: Internatl. symposium on Water-Rock Interaction, Czechoslovakia, 1974, Proc., p. 158-169.

Helgeson, H. C., 1967, Solution chemistry and metamorphism, *in* Abelson, P. H., ed., Researches in Geochemistry, v. 2: New York, John Wiley & Sons, p. 362-404.

———— 1968, Geologic and thermodynamic characteristics of the Salton Sea geothermal system: Am. Jour. Sci., v. 266, p. 129-166.

———— 1969, Thermodynamics of hydrothermal systems at elevated temperatures and pressures: Am. Jour. Sci., v. 267, p. 729-804.

———— 1981, Prediction of the thermodynamic properties of electrolytes at high pressures and temperatures, *in* Wickman, F. and Rickard, D., eds., Chemistry and Geochemistry of Solutions at High Temperatures and Pressures: Royal Swedish Acad. Sci., Stockholm, in press.

Helgeson, H. C., and Kirkham, D. H., 1974a, Theoretical prediction of the thermodynamic behavior of aqueous electrolytes at high pressures and temperatures. I. Summary of the thermodynamic/electrostatic properties of the solvent: Am. Jour. Sci., v. 274, p. 1089-1198.

———— 1974b, Theoretical prediction of the thermodynamic behavior of aqueous electrolytes at high pressures and temperatures. II. Debye-Huckel parameters for activity coefficients and relative partial molal properties: Am. Jour. Sci., v. 274, p. 1199-1261.

———— 1976, Theoretical prediction of the thermodynamic behavior of aqueous electrolytes at high pressures and temperatures: III. Equation of state for aqueous species at infinite dilution: Am. Jour. Sci., v. 276, p. 97-240.

Helgeson, H. C., Kirkham, D. H., and Flowers, G. C., 1981, Theoretical prediction of the thermodynamic behavoir of aqueous electrolytes at high pressures and temperatures. IV. Calculation of activity coefficients, osmotic coefficients, and apparent molal and standard and relative partial mole properties to 5 kb and 600°C: Am. Jour. Sci., v. 281, in press.

Helgeson, H. C., Delany, J. M., Nesbitt, H. W., and Bird, D. K., 1978, Summary and critique of the thermodynamic properties of rock-forming minerals: Am. Jour. Sci., v. 278-A, 229 p.

Hoagland, J. R., and Elders, W. A., 1978, Hydrothermal mineralogy and isotopic geochemistry in the Cerro Prieto geothermal field, Mexico. I. Hydrothermal mineral zonation: Geothermal Resources. Council Trans., v. 2, p. 283-286.

Holdaway, M. J., 1965, Basic regional metamorphism in part of the Klamath Mountains, Northern California: Am. Mineralogist, v. 50, p. 953-977.

———— 1972, Thermal stability of aluminum-iron epidote as a function of f_{O_2} and iron content: Contr. Mineralogy Petrology, v. 36, p. 307-340.

Hörmann, P.-K., and Raith, M., 1973, Bildungsbedingungen von Al–Fe(III)–epidote: Contr. Mineralogy Petrology, v. 38, p. 307-320.

Höy, T., 1976, Calc–silicate isograds in the Riondel area, southeastern British Columbia: Canadian Jour. Earth Sci., v. 13, p. 1093-1104.

Keith, T. E. C., Muffler, L. J. P., and Cremer, M., 1968, Hydrothermal epidote formed in the Salton Sea geothermal system, California: Am. Mineralogist, v. 53, p. 1653-1644.

Kendall, C., ms, 1976, Petrology and stable isotope geochemistry of three wells in the Buttes area of the Salton Sea Geothermal Field, Imperial Valley, California, U.S.A.: M.S. thesis, Univ. California, Riverside, Calif.

Kerrick, D. M., 1977, The genesis of zoned skarns in the Sierra Nevada, California: Jour. Petrology, v. 18, p. 144-181.

Kerrick, D. M., and Darken, L. S., 1975, Statistical thermodynamic models for ideal oxide and silicate solid solutions, with application to plagioclase: Geochim. et Cosmochim. Acta, v. 39, p. 1431-1442.

Kerrick, D. M., and Jacobs, G. K., 1978, Experimental and thermodynamic analysis of decarbonation equilibria in P–T–X_{CO_2} space [abs.]: Am. Geophys. Union Trans., v. 59, no. 4, p. 402.

Kretz, R., 1963, Note on some equilibria in which plagioclase and epidote participate (discussion): Am. Jour. Sci., v. 261, p. 973-982.

Lindh, Anders, 1978, Aspects on plagioclase–epidote thermometry: Neues Jabr. Mineralogie Abh., v. 133, p. 113-131.

Liou, J. G., 1971, Synthesis and stability of prehnite, $Ca_2Al_2Si_3O_{10}(OH)_2$: Am. Mineralogist, v. 56, p. 507-531.

McDowell, D., and Elders, W. A., 1978, Distribution and chemistry of layer-silicate minerals in the Salton Sea geothermal field, California [abs.]: Geol. Soc. America, Abs. with Programs, v. 3, p. 452-453.

McDowell, D., and McCurry, M., 1977, Active-metamorphism in the Salton Sea Geothermal Field, California: Mineralogical and mineral chemical changes with depth and temperature in sandstone [abs.]: Geol. Soc. America, Abs. with Programs, v. 9, p. 1088.

McKenzie, W. F., and Helgeson, H. C., 1979, Calculation of the dielectric constant of H_2O and the thermodynamic properties of aqueous species at temperatures to 900°C [abs.]: Geol. Soc. America, Abs. with Programs, v. 11, p. 476.

———— 1980, Calculated phase relations among silicates, copper iron sulfides, and aqueous solutions at magmatic temperatures [abs.]: Geol. Soc. America, Abs. with Programs, v. 12, p. 481.

Misch, Peter, 1968, Plagioclase compositions and non-anatectic origin of migmatitic gneisses in Northern Cascade Mountains of Washington State: Contr. Mineralogy Petrology, v. 17, p. 1-70.

Miyashiro, A., and Seki, Y., 1958, Enlargement of the composition field of epidote and piemonite with rising temperature: Am. Jour. Sci., v. 256, p. 423-430.

Morteani, G., and Raase, P., 1974, Metamorphic plagioclase crystallization and zones of equal anorthite content in epidote-bearing, amphibole-free rocks of the western Tauernfenster, eastern Alps: Lithos, v. 7, p. 101-111.

Muffler, L. J. P., and White, D. W., 1969, Active metamorphism of Upper Cenozoic sediments in the Salton Sea geothermal field and the Salton Trough, Southeastern California: Geol. Soc. America Bull., v. 80, p. 157-182.

Nissen, H.-U., 1974, Exsolution phenomena in bytownite plagioclase, *in* Mackenzie, W. S., and Zussman, J., eds., The Feldspars: Manchester, England, Manchester Univ. Press, p. 491-521.

Noble, D. C., 1962, Plagioclase unmixing and the lower boundary of the amphibolite facies: Jour. Geology, v. 70, p. 234-240.

Noboko, S. I., 1970, Facies of hydrothermally altered rocks of Kamchatka-Kurile volcanic arc: Pacific Geology, v. 2, p. 23-27.

———— 1976, The origin of hydrothermal solutions and related propylitization and argillization in the areas of tectonomagmatic activity: Internat. Symposium on Water-Rock Interaction, Czechoslovakia, 1974, Proc., p. 184-195.

Orville, P. M., 1972, Plagioclase cation exchange equilibria with aqueous chloride solution: results at 700°C and 2000 bars in the presence of quartz: Am. Jour. Sci., v. 272, p. 234-272.

———— 1974, The "peristerite gap" as an equilibrium between ordered albite and disordered plagioclase solid solution: Soc. franç Mineralogie cristallographie bull., v. 97, p. 386-392.

Orville, P. M., and Johannes, W., 1972, The composition of plagioclase as an indicator of metamorphic grade and fluid composition in carbonate-bearing pelitic rocks [abs.]: Internat. Geol. Cong. 24th, Montreal 1972, Proc., Sec. 2, p. 3.

Perchuk, L. L., and Aranovich, L. Ya., 1979, Thermodynamics of minerals of variable composition: Andradite–grossularite and pistacite–clinozoisite solid solutions: Phys. Chem. Minerals, v. 5, p. 1-14.

Perkins, D., III, Westrum, E. F., Jr., and Essene, E. J., 1980, The thermodynamic properties and phase relations of some minerals in the system CaO–Al_2O_3–SiO_2–H_2O: Geochim. et Cosmochim. Acta., v. 44, p. 61-84.

Raith, M., 1976, The Al–Fe (III) epidote miscibility gap in a metamorphic profile through the Penninic series of the Tauern window, Austria: Contr. Mineralogy Petrology, v. 57, p. 99-117.

Rambaldi, E. R., 1973, Variation in the composition of plagioclase and epidote in some metamorphic rocks near Bancroft, Ontario: Canadian Jour. Earth Sci., v. 10, p. 852-868.

Ramberg, H., 1943, En undersøkelse av. Vestrandens regionalmetamorfe kergartee: Norsk Geol. Tidsskr., v. 23, p. 1-174.

———— 1944, Petrological significance of sub-solidus phase transitions in mixed crystals: Norsk Geol. Tidsskr., v. 24, p. 42-74.

———— 1949, The facies classification of rocks: a clue to the origin of quartzo–feldspathic massifs and veins: Jour. Geology, v. 57, p. 18-54.

———— 1952, The origin of metamorphic and metasomatic rocks: Chicago, Ill., Univ. Chicago Press, 317 p.

Rosenqvist, I. Th., 1952, The metamorphic facies and the feldspar minerals, Univeritetet i Bergen, Arbok, 1952, Naturvitenskapelig rekke, Nr. 4, p. 108.

Rutland, R. W. R., 1961, The control of anorthite content of plagioclase in metamorphic crystallization (discussion): Am. Jour. Sci., v. 259, p. 76-79.

———— 1962, Feldspar structure and the equilibrium between plagioclase and epidote (a reply): Am. Jour. Sci., v. 260, p. 153-157.

Saxena, S. K., and Ribbe, P. H., 1972, Activity-composition relations in feldspars: Contr. Mineralogy Petrology, v. 37, p. 131-138.

Seki, Y., 1972, Lower-grade stability limit of epidote in light of natural occurrences: Geol. Soc. Japan Jour., v. 78, p. 405-413.

Sen, S. R., 1963, Some consequences of ordering and unmixing in sodic plagioclases on epidote–plagioclase equilibrium in regionally metamorphosed rocks (discussion): Am. Jour. Sci., v. 261, p. 786-780.

Steck, A., 1976, Albit–oligoklas–mineralgesellschaften der peristeritlücke aus alpinmetamorphen granitgneisen der Gotthardmassivs: Schweizer. min. pet. Mitt., v. 56, p. 269-292.

Steiner, A., 1953, Hydrothermal rock alteration at Wairakei, New Zealand: Econ. Geology, v. 48, p. 1-13.

———— 1968, Clay minerals in hydrothermally altered rocks at Wairakei, New Zealand: Clays and Clay Minerals, v. 16, p. 193-213.

Strens, R. G. J., 1965, Stability-relations of Al–Fe epidotes: Mineralog. Mag., v. 35, p. 464-475.

Turner, F. J., 1948, Evolution of the metamorphic rocks: Geol. Soc. America Mem. 30, 342 p.

———— 1968, Metamorphic Petrology: New York, McGraw-Hill, Inc., 403 p.

Walther, J. V., and Helgeson, H. C., 1977, Calculation of the thermodynamic properties of aqueous silica and the solubility of quartz and its polymorphs at high pressures and temperatures: Am. Jour. Sci., v. 277, p. 1315-1351.

———— 1980, Description and interpretation of metasomatic phase relations at high pressures and temperatures: I. Equilibrium activities of ionic species in nonideal mixtures of CO_2 and H_2O: Am. Jour. Sci., p. 575-606.

Wenk, E., 1962, Plagioklas als indexmineral in den Zentralalpen: Schweizer. min. pet. Mitt., v. 41, p. 311-319.

Wenk, E., and Keller, F., 1969, Isograde in Amphibolitserien der Zentralalpen: Schweizer. min. pet. Mitt., v. 49, p. 159-198.

Wenk, E., and Wenk, H. R., 1977, An-variation and intergrowths of plagioclases in banded metamorphic rocks from Val Carrechio (Central Alps): Schweizer. min. pet. Mitt., v. 57, p. 41-57.

Wenk, E., Wenk., H.-R., Glauser, A., and Schwander, H., 1975, Intergrowth of andesine and labradorite in marbles of the central Alps: Contr. Mineralogy Petrology, v. 53, p. 311-326.

Wenk, H.-R., 1977, Metamorphic plagioclase, occurrence and variation [abs.]: Am. Geophys. Union Trans., v. 58, no. 6, p. 521-522.

White, D. E., and Sigvaldason, G. E., 1961, Epidote in hot-spring systems, and depth of formation of propylitic epidote in epithermal ore deposits: U.S. Geol. Survey Prof. Paper, v. 450-E, p. 80-84.

Windom, K. E., and Boettcher, A. L., 1976, The effect of reduced activity of anorthite on the reaction grossular + quartz = anorthite + wollastonite: a model for plagioclase in the earth's lower crust and upper mantle: Am. Mineralogist, v. 61, p. 886-896.

Winkler, H. G. F., 1974, Petrogenesis of metamorphic rocks: New York, Springer-Verlag, 320 p.